

**FEDERAL HIGHWAY ADMINISTRATION
TURNER-FAIRBANK HIGHWAY RESEARCH CENTER REPORT**

***Mechanical Property Test Report
(I-35W over the Mississippi River)***

October 15, 2008

**Fassil Beshah, Ph.D.
Federal Highway Administration**

**William Wright, Ph.D., P.E.
Federal Highway Administration**

**Benjamin Graybeal, Ph.D., P.E.
Federal Highway Administration**

TABLE OF CONTENTS

1.0	BACKGROUND	3
2.0	U10 GUSSET PLATE TESTS	4
2.1	Gusset Plate Tension Tests	6
2.2	Charpy V-Notch Impact Tests	10
2.3	Compact Tension Tests	14
3.0	MEMBER TENSION TESTS	18
4.0	DECK AND PIER CONCRETE CORE TESTS	24
	REFERENCES	27
APPENDIX A	Specimen Marking and Cut Plan for the U-10 Gusset Plates	28
APPENDIX B	Stress-Strain Curves for the U-10 Gusset Plate Tension Tests	34
APPENDIX C	Compact Tension Test Results for the U-10 Gusset Plates	43

1.0) BACKGROUND

I-35W Bridge which carried I-35W highway over the Mississippi River was located in Minneapolis, Minnesota. The bridge was open for traffic in November 1967 and failed on August 1, 2007. It was three-span continuous (256 - 456 - 256 ft) deck truss with multiple approach spans to the north and south. The bridge cross-section consisted of two main trusses spaced at 72 feet 4 inches, as shown in figure 1.

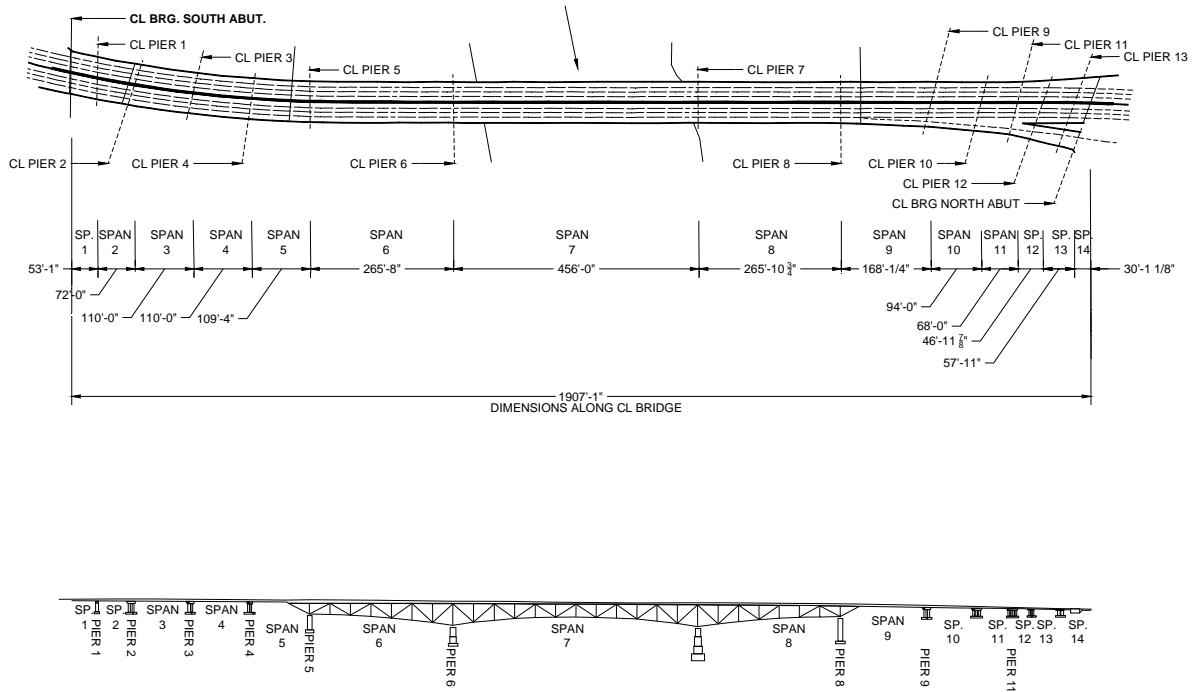


Figure 1 Plan view and elevation of I-35W bridge.

The collapse investigation quickly focused on the U-10 location in the main span of the deck truss as a possible initiating point for the failure. The U-10 joints are located along the upper truss chord, two panel points north of pier 6, in span 7 of the main truss. The gusset plates at the U-10 locations in both the east and west trusses were observed to be bent and fractured in the wreckage. The purpose of this report is to determine the mechanical properties of the steel and concrete in the bridge with a particular emphasis on the steel in the U-10 gusset plates and the surrounding truss members. This information is intended to assess the general quality of the material and provide input data for the analytical modeling effort to investigate the bridge collapse.

2.0) U-10 GUSSET PLATE TESTS

There are four separate gusset plates that failed at the U-10 location, two in the east truss and two in the west. For the remainder of this report, the gusset plates are identified for each truss (east or west) and each side of the joint (east or west). For example, gusset plate U10W-E is the plate on the east side of the U10 joint in the west truss. This nomenclature is used to identify all of the specimens tested in this report. The first two letters of each specimen ID refers to the truss (E or W) and the side of the joint (E or W).

The U-10 gusset plates were specified to be manufactured from ASTM A441 steel with the minimum specified yield strength of 50 ksi (345 MPa) and a minimum ultimate strength of 65 ksi (450 MPa). The plates all have a nominal thickness of ½ in. (13mm). Figure 2 shows the sections that were removed from the wreckage for testing. The plates were removed from an area where the gusset plates were intact and still attached to the top chord member of the truss. The rivet heads were carefully ground off and the plates were removed without introducing any damage. The sample location was carefully chosen to obtain material with no apparent damage due to the collapse. Once removed, the plates were shipped to the FHWA Turner-Fairbank Highway Research Center (TFHRC) in McLean, Virginia for testing.

Test specimens were cut from each plate according to the layout shown in Appendix A. Since the gusset plates are approximately square in shape, the rolling direction could not be easily determined based on orientation in the bridge. The fabricator may have arbitrarily laid-out the plate cutting to minimize waste in the cutting process. All of the test specimens are laid-out and identified relative to the direction from which they were removed from the plate. Longitudinal refers to the north-south direction in the bridge. Transverse refers to the up-down direction. These directions relate directly to the damage planes existing in the wreckage but may not correspond to the rolling direction of the plate.

Three different tests were performed to determine the strength and toughness properties of the gusset plate material. Tension tests were performed to determine the yield strength, tensile strength, and ductility of the steel. A series of Charpy-Vee-Notch (CVN) tests were performed to determine plate toughness relative to the current AASHTO Material Specifications. The CVN test is commonly used for quality control in steel production, but it cannot directly be used to determine fracture resistance. No toughness criteria existed for bridge steels when the I-35W bridge was constructed, but a comparison can be made to modern specifications. Finally, a series of compact tension (C(T)) tests were performed to determine the fracture resistance of the plate under conditions that were present at the time of collapse. The C(T) test results can be directly used to predict the elastic-plastic fracture resistance and tearing resistance of the plate in the presence of a crack.

The layout of the individual test specimens and their geometry are shown in Appendix A for each of the four plates tested. The first two letters in each specimen ID code relate to the truss (E or W) and the side of the joint (E or W). The third letter refers to the direction in the plate (L or T) for which the properties are being determined. For the tension tests, this

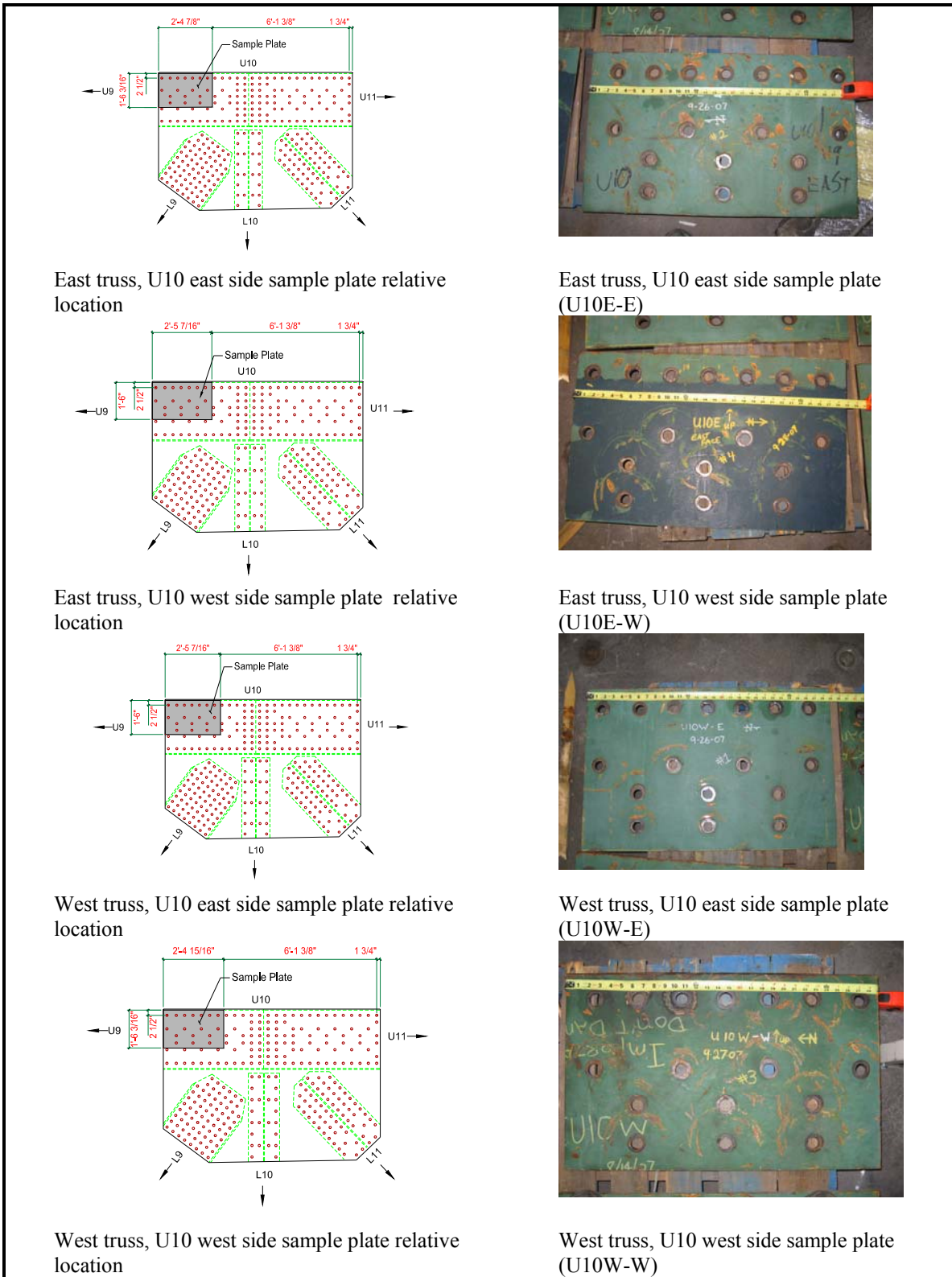


Figure 2 Location of the steel plates removed from the U10 gussets for material property testing.

relates to the strength of the plate pulled in either the longitudinal or transverse direction. For the toughness tests, this relates to the fracture resistance of the plate with a crack growing transverse to either the longitudinal or transverse directions.

2.1) Gusset Plate Tension Tests

All testing was performed in accordance with the ASTM E8 Standard Test Methods for Tension Testing of Metallic Materials. The E8 standard defines the methods and procedures that were used to determine yield strength, yield point elongation, tensile strength, percent elongation, and area reduction. In addition, load and elongation data was digitally collected during the test to develop the stress-strain relationship for the steel in tension.

The standard plate-type tension specimen with an 8 in. gage length was utilized for all testing. The specimen is fabricated from the full thickness of the plate, thereby averaging out any through thickness variability that may exist. The specimens were fabricated with a slightly thinner width in the center (0.1%) to induce failure within the gage length of the specimen. All specimens were tested in an MTS 110-kip hydraulic testing machine equipped with hydraulic wedge grips as shown in figure 3. A 110-kip load cell recorded load data and an MTS extensometer with an 8 in. gage length and 1.0 in. travel range was attached to the specimens to measure elongation.

In the elastic testing region, each specimen was loaded at a constant rate of 0.02 in/min, corresponding to roughly 22 ksi/min. The yield strength determined by the ASTM test method is somewhat dependent on the rate of testing, with higher test rates resulting in higher yield strength. The rate for the tests in this report is close to the lower bound allowed by ASTM, therefore providing a conservative estimate of yield strength. Experience has shown that testing at the ASTM maximum of 100 ksi/min will result in yield strengths that are about 2 percent higher. The E8 testing procedure was supplemented with procedures specified in the Structural Stability Research Council (SSRC) Technical Memorandum No. 7 to determine static yield strength. The cross head displacement is held constant for several five minute hold periods once the specimen is on the yield plateau. The minimum load at the end of the hold periods is used to determine the static yield strength. Once the specimen begins to undergo strain hardening, the load rate is increased to provide a displacement of 0.6 in. / min. The extensometer was removed from the specimen prior to failure once it reached the travel limit of 1.0 in. This was past the point where the ultimate load occurred during the test. However, the descending portion of the stress-strain curve could not be recorded. The total elongation and reduction in area was physically measured from the broken specimens after testing.

Data from the load cell and the extensometer were used to recreate the engineering stress-strain curves shown in Appendix B. Figure 4 shows a typical stress-strain curve for the material. The results appear typical for grade 50 structural steel. Following the initial elastic portion of the curve, a significant yield plateau is observed followed by a long region of strain hardening before the tensile strength is reached. Note that the stress-strain curve is truncated prior to failure since the elongation exceeds the working range of the extensometer.



Figure 3 Gusset plate tension test using MTS self-aligning grips and extensometer with an 8 in. gage length.

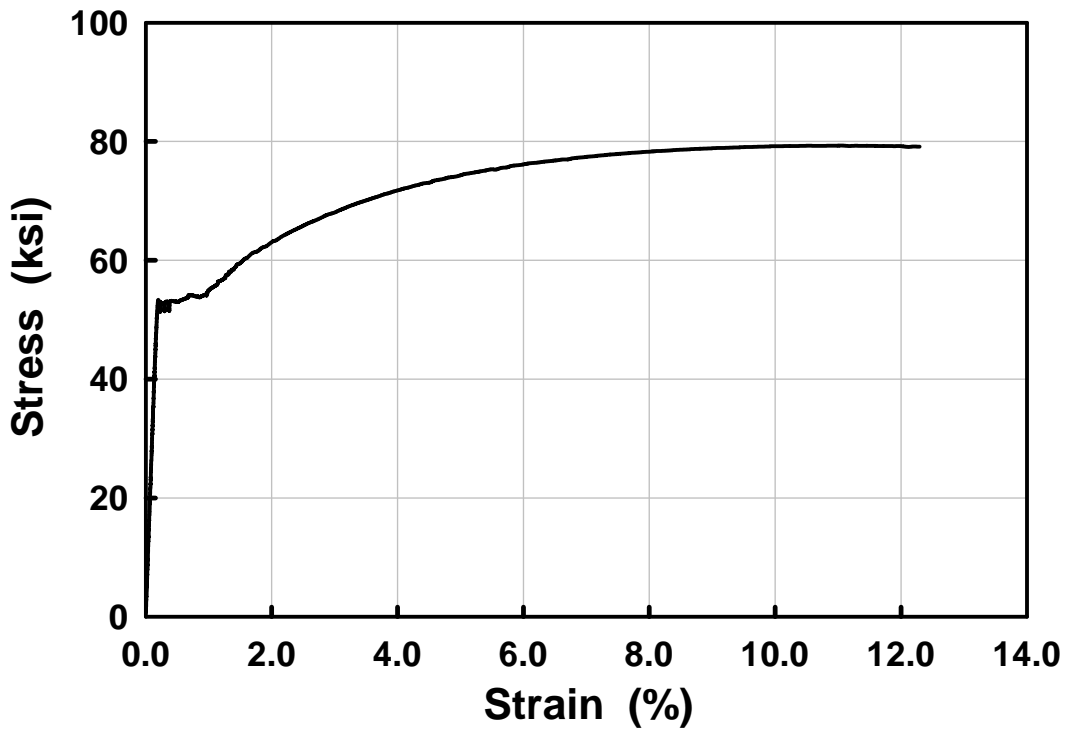


Figure 4 Typical stress-strain curve for the U10 gusset plate material (specimen WE-L2).

Table 1 summarizes the tension test results for the U10 gusset plates. All of the tests exceeded the minimum specified yield strength of 50 ksi for A441 steel. As expected, there is low variability between the two replicate tests at each sample location. The average strength for each test location is also reported. On average, the static yield strength was about 2.6 percent lower than the 0.2% offset yield strength.

Table 1 Summary of Gusset Plate Tension Test Results.

Specimen I.D.	0.2% Offset Yield Strength		Static Yield Strength		Tensile Strength	Elongation (%)	Area Reduction (%)
	ϵ_y (%)	F_y (ksi)	ϵ_y (%)	F_y (ksi)	F_u (ksi)		
Longitudinal Direction							
WE-L1	0.39	52.50	0.38	51.15	80.40	22.43	59.11
WE-L2	0.38	53.07	0.37	51.54	79.34	23.44	59.00
Avg.	0.38	52.78	0.38	51.35	79.87	22.94	59.05
WW-L1	0.38	52.94	0.37	51.41	78.85	23.07	59.37
WW-L2	0.38	50.21	0.37	49.42	76.26	22.67	59.79
Avg.	0.38	51.58	0.37	50.42	77.56	22.87	59.58
EW-L1	0.38	52.11	0.38	50.61	79.77	22.89	58.85
EW-L2	0.38	51.65	0.38	50.53	79.36	22.26	57.85
Avg.	0.38	51.88	0.38	50.57	79.57	22.57	58.35
EE-L1	0.38	53.74	0.37	52.19	81.84	22.57	57.72
EE-L2	0.38	53.78	0.37	51.52	81.21	21.89	60.16
Avg.	0.38	53.76	0.37	51.85	81.53	22.23	58.94
Transverse Direction							
WE-T1	0.38	54.41	0.38	52.94	81.52	19.98	50.97
WE-T2	-	-	-	-	-	-	-
Avg.	0.38	54.41	0.38	52.94	81.52	19.98	50.97
WW-T1	0.38	54.39	0.38	52.86	84.36	19.98	51.18
WW-T2	0.38	51.54	0.38	50.43	77.48	18.44	53.73
Avg.	0.38	52.96	0.38	51.65	80.92	19.21	52.45
EW-T1	0.38	52.03	0.37	50.60	79.66	18.42	51.60
EW-T2	0.38	53.63	0.37	52.22	80.30	16.40	49.51
Avg.	0.38	52.83	0.37	51.41	79.98	17.41	50.56
EE-T1	0.38	54.44	0.38	53.16	81.90	16.96	49.36
EE-T2	0.39	53.88	0.39	52.40	81.26	17.21	50.36
Avg.	0.39	54.16	0.38	52.78	81.58	17.08	49.86

2.2) Charpy V-Notch Impact Tests

Charpy V-notch (CVN) specimens were tested for each gusset plate in accordance with the procedure described in ASTM E23. For each plate, a standard CVN test consisting of three replicate specimens was performed in both the longitudinal (L-T) and transverse (T-L) directions in the plates. A test temperature of +50°F (+10°C) was maintained for all tests.

A Physonet Charpy Impact Test Machine with a 128 ft-lb. maximum capacity was utilized for testing. The machine was examined at the beginning of the testing program and found to comply with ASTM E23 sections 5 and 6. ASTM E23 Section 6.2.6.2 outlines the windage and friction test procedure. Friction loss per pendulum swing was checked and was found to be within the specified maximum of 0.40% of the scale range. The test was performed using a standard Type A Charpy (Simple-Beam) Impact Test Specimen. The required dimensions and permissible tolerances specified by ASTM E23 are shown in Figure A5.

Before each specimen was tested, it was placed and immersed in methanol by using FTS Systems, Inc. Multi-Cool low-temperature bath. The bath temperature was monitored by a thermocouple. Each specimen was conditioned in the bath for at least five minutes prior to testing. A temperature of +50°F was maintained within $\pm 1^\circ\text{F}$ for all specimens. Self-centering tongs were used to load the specimens from the bath to the testing machine. The tongs were also cooled in the bath along with the specimens. The total elapsed time from specimen removal to testing was no greater than five second conforming to ASTM procedures. The CVN energy was determined from the pendulum rebound recorded during testing. Lateral expansion was measured according to ASTM procedures. The percent shear area was determined from digital photographs that were imported into AutoCAD.

The entire lot of longitudinal (L-T) specimens remained intact following fracture. The energy absorbed by these specimens did not exceed 80% of the machine capacity. Lateral expansion and percent shear area measurements for these specimens were inconsequential, therefore they are not reported.

The CVN test results are listed in table 2 and are plotted in figures 5 and 6. The amount of scatter between the three replicate specimens at each test location appears typical for grade 50 structural steel. For each test orientation, the test results were relatively consistent between each of the four gusset plates tested. However, there is a noticeable difference in toughness between the longitudinal (L-T) and transverse (T-L) specimens for all four plates. Figures 5 and 6 show an average test result of 61 ft-lb@50 F for the L-T orientation compared to 29 ft-lb@50 F for the T-L orientation.

The I-35W bridge was constructed before AASHTO adopted CVN requirements for bridge steels. For temperature zone 2 (lowest anticipated service temperature = -30 F), the current AASHTO code requires 25 ft-lb@+40 F for fracture critical applications with testing to be performed on each individual plate or shape ("P" frequency). For non-fracture critical applications the specifications require 15 ft-lb@+40 F sampled once for each heat of steel

("H" frequency). The ASTM A 673 specification requires the longitudinal axis of the CVN specimens to be parallel to the rolling direction of the plate (L-T orientation) for testing structural plate. Despite the 10 F difference in test temperature between the present tests and the zone 2 specification temperature, it is clear that the gusset plate material in the L-T orientation would have met the modern CVN requirements for zone 2, fracture critical use. The transverse toughness, however, would have been marginal for zone 2, fracture critical use and any given test might pass or fail depending on the inherent variability of testing. However, since transverse toughness testing is not required by the A 709 specification, the toughness cannot be considered deficient based on the specification.

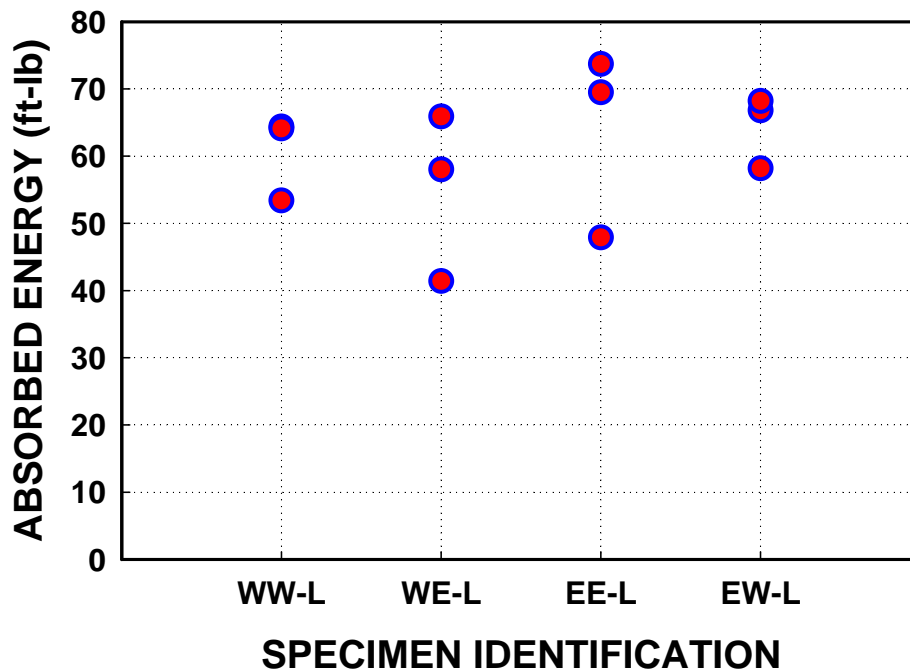


Figure 5 Absorbed energy for longitudinal specimens (L-T) at +50 F (+10 C).

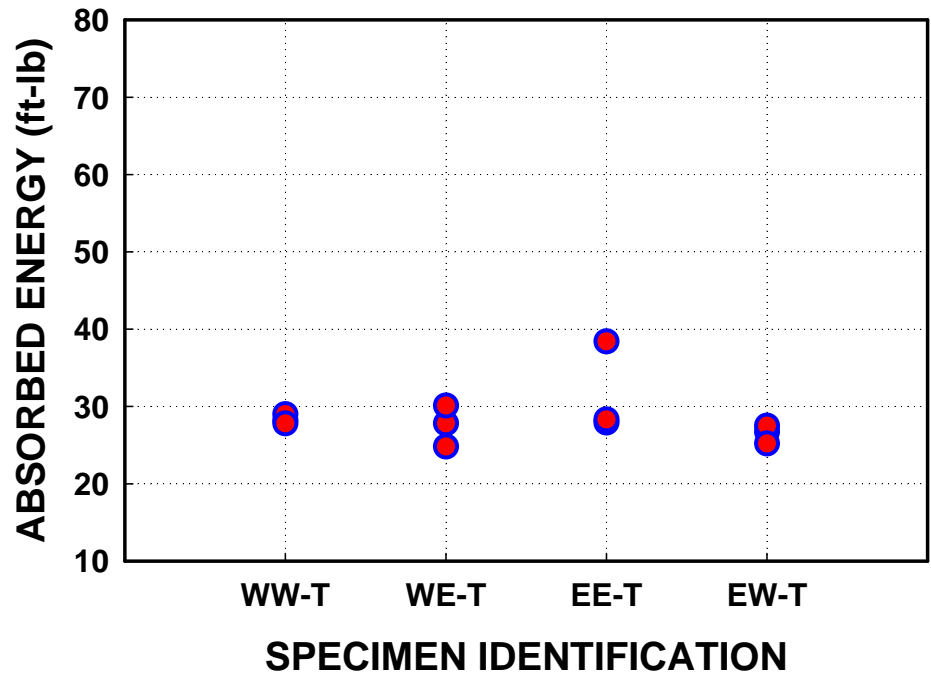


Figure 6 Absorbed energy for transverse specimens (T-L) at +50°F (+10 C).

Table 2 Charpy Vee-Notch Results from Gusset Plate Samples.

PLATE	ORIENTATION (a, b)	SPECIMEN ID	ABSORBED ENERGY		LATERAL EXPANSION (in)	PERCENT SHEAR (%)
			Individual (ft-lb@+50°F)	Average (ft-lb@+50°F)		
WW	L-T	WW-L1	64.4	60.6	-	-
		WW-L2	53.4		-	-
		WW-L3	64.1		-	-
	T-L	WW-T1	28.3	28.4	0.13	55
		WW-T2	29.0		0.14	55
		WW-T3	27.8		0.11	55
WE	L-T	WE-L1	41.4	55.1	-	-
		WE-L2	65.9		-	-
		WE-L3	58.0		-	-
	T-L	WE-T1	27.8	27.6	0.14	57
		WE-T2	30.1		0.14	54
		WE-T3	24.8		0.12	56
EW	L-T	EW-L1	58.2	64.4	-	-
		EW-L2	66.8		-	-
		EW-L3	68.2		-	-
	T-L	EW-T1	26.7	26.5	0.13	54
		EW-T2	27.5		0.14	55
		EW-T3	25.2		0.11	59
EE	L-T	EE-L1	47.9	63.7	-	-
		EE-L2	69.5		-	-
		EE-L3	73.7		-	-
	T-L	EE-T1	27.9	31.5	0.12	61
		EE-T2	38.4		0.16	49
		EE-T3	28.3		0.12	61

- a) First letter indicates direction normal to crack plane, second letter indicates direction of crack propagation.
b) It is assumed that the gusset plates are oriented with the rolling direction in the north-south direction.

2.3) Compact Tension Tests

Twelve compact tension (C(T)) tests were performed to determine the tearing resistance of the plates at the time of the collapse. The C(T) tests were all performed at room temperature (about 75 F) to measure material toughness under conditions close to those at the time of collapse of the bridge (about 90 F). Since the test results showed ductile, upper shelf behavior at 75 F, no additional toughness would be expected for increased testing temperatures. Therefore, no attempt was made to heat the specimens prior to testing. All testing was performed according to the ASTM E 1820-08 Standard Test Method for Measurement of Fracture Toughness. An MTS 22 kip servo-hydraulic test frame was utilized with standard clevis-type grips for C(T) testing.

Similar to the CVN tests, the specimens were tested with the cracks oriented in the longitudinal (L-T) and transverse (T-L) directions. The layout of the C(T) specimens is shown in Appendix A. Figure 7 shows the results from two typical C(T) tests. The upper plot shows the basic load versus displacement data recorded by the clip gage during testing. The slope of the periodic unloading lines are measured and used to determine the crack length at any given point in the test. The lower plot shows a J-R curve indicating the resistance of the specimens to ductile crack extension. The dashed lines show the validity limits for data specified in the E 1820 specification. The J-R curve shown in the lower plot is a power law regression fit to the data inside the validity box. The data outside the box is included to show the behavior trend after a significant amount of crack extension occurs. Note that two different tests are shown in figure 7, one in the longitudinal and one in the transverse direction. Figures showing the results from each individual specimen are shown in Appendix C. No fracture instability was observed in any of the C(T) tests, indicating that the mode of failure is stable ductile tearing. However, there is a noticeable difference between the shape of the curves between the transverse and longitudinal directions. The results from all specimens in a given orientation are very similar for all four gusset plates tested.

Because the fracture behavior was fully ductile, no attempt was made to analyze fracture in terms of the linear elastic parameter K_{Ic} . The resistance to the onset of stable crack extension is defined as J_{Ic} . The J_{Ic} results listed in table 3 and shown in figure 8 cannot be considered valid according to the procedures set forth in ASTM E 1820. One or more of the ASTM qualification criteria failed for each specimen. This parameter is very sensitive to minor variations in the data and the results plotted in figure 8 show a large degree of scatter. Although not valid, the J_{Ic} results could be used to assist in fracture analysis of the gusset plates in terms of the J-Integral.

An alternative method of predicting ductile fracture resistance is comparing the load capacity of the specimen to the calculated limit load based on the yield strength of the material. Previous work has shown that this is a good predictor of ductile fracture in I-girders (Wright et.al. 2006). Figure 9 shows the a plot of the maximum load achieved during testing (P_{max}) normalized by the limit load capacity of the C(T) specimen based on yield

Table 3 Ductile Fracture Test Results.

Specimen	Tensile Properties				Fracture Results		
	E (ksi x 10 ⁶)	v	σ_{YS} (ksi)	σ_{TS} (ksi)	P_{max} (lbs)	$P_{L,YS}$ (lbs)	$J_{Ic}^{(a)}$ (in-lb/in ²)
EE-L1	29.7	0.29	53.76	81.53	5890	5283	1507
EE-L2					6115	5485	759
EE-T1			54.16	81.58	4923	5171	617
EE-T2					5283	5328	799
EW-L1			51.88	79.57	6632	6182	1302
EW-L2					6407	6025	919
EW-T1			52.83	79.98	4766	5440	468
EW-T2					4811	6025	668
WW-L1			51.58	77.56	5485	5373	1125
WW-L2					6205	6047	788
WW-T1			52.96	80.92	5126	5395	502
WW-T2					4429	4519	885
WE-L1			52.78	79.87	5823	5485	1256
WE-L2					6025	5530	1142
WE-T1			54.41	81.52	5373	5440	388
WE-T2					5440	5643	502

a) All J_{Ic} results are failing one or more of the ASTM validity criteria, therefore these cannot be considered valid results.

strength. Values exceeding 1.0 indicate a fully ductile tearing mode of failure. Values below 1.0 indicate somewhat reduced ductile fracture resistance. For reference, brittle steels typically can only reach values of about 1/3 $P_{L,YS}$ before fracture.

In general, there is a clear directionality associated with the fracture results. The gusset plates have significantly higher ductile fracture resistance in the longitudinal direction compared to the transverse direction. This is clearly shown in figure 7 comparing the J-R curves for the two directions. This is also shown in terms of J_{Ic} and limit load analysis shown in figures 8 and 9. Likewise, this is consistent with the CVN results shown in the previous section that show a lower toughness in the transverse direction. However, by all accounts the gusset plates are failing by ductile tearing, not brittle fracture. This is consistent with observations of the fractures that occurred in the bridge wreckage that showed significant ductility and necking prior to fracture.

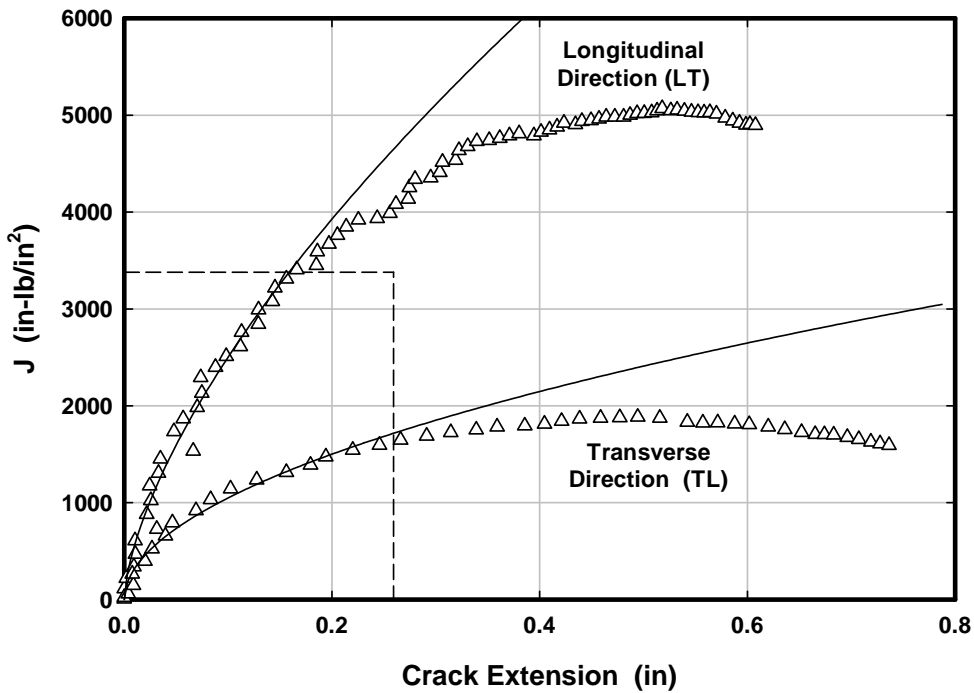
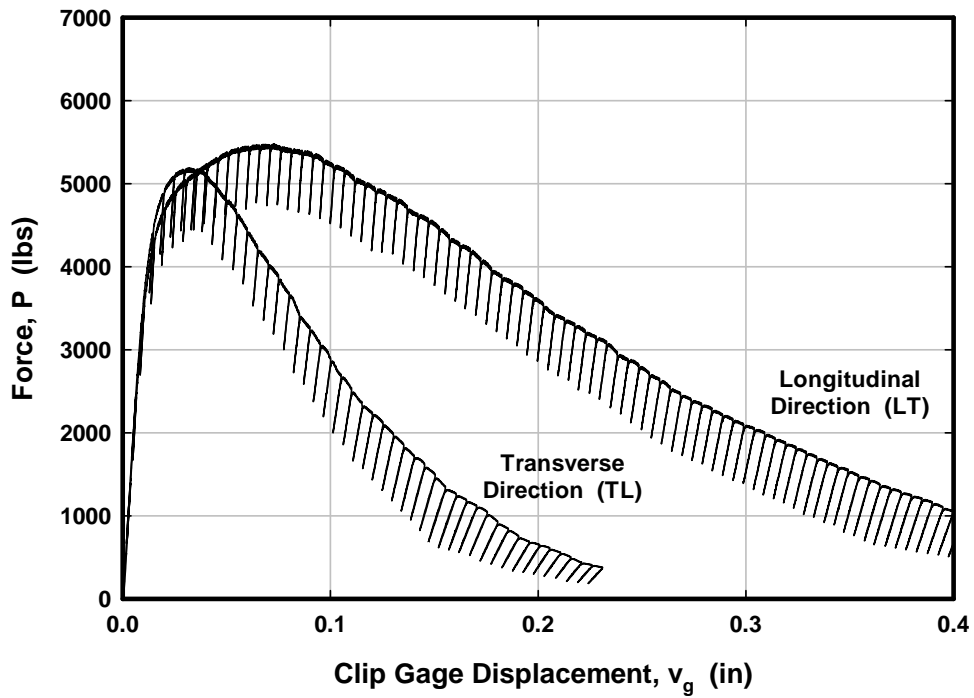


Figure 7 Typical C(T) test results comparing the fracture resistance in the longitudinal direction to the transverse direction . These results are based on specimens WW-L1 and WW-T1. The top plots show the basic load versus clip gage displacement recorded during the test. The bottom plots show the J-R curves constructed to show the resistance to stable ductile crack extension.

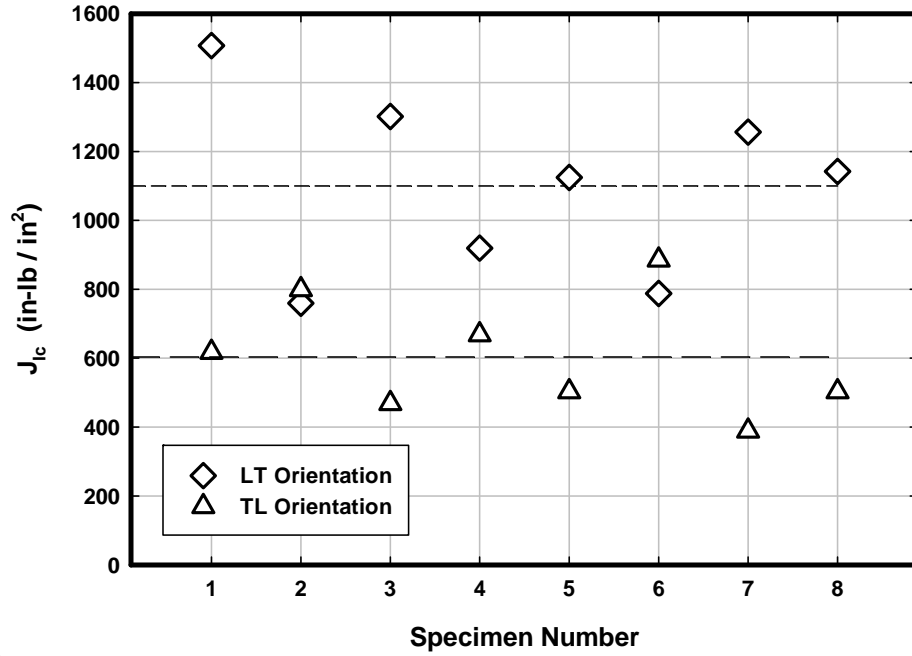


Figure 8 Estimated J_{1c} at the start of stable crack extension. (These values do not meet all of the ASTM validity criteria)

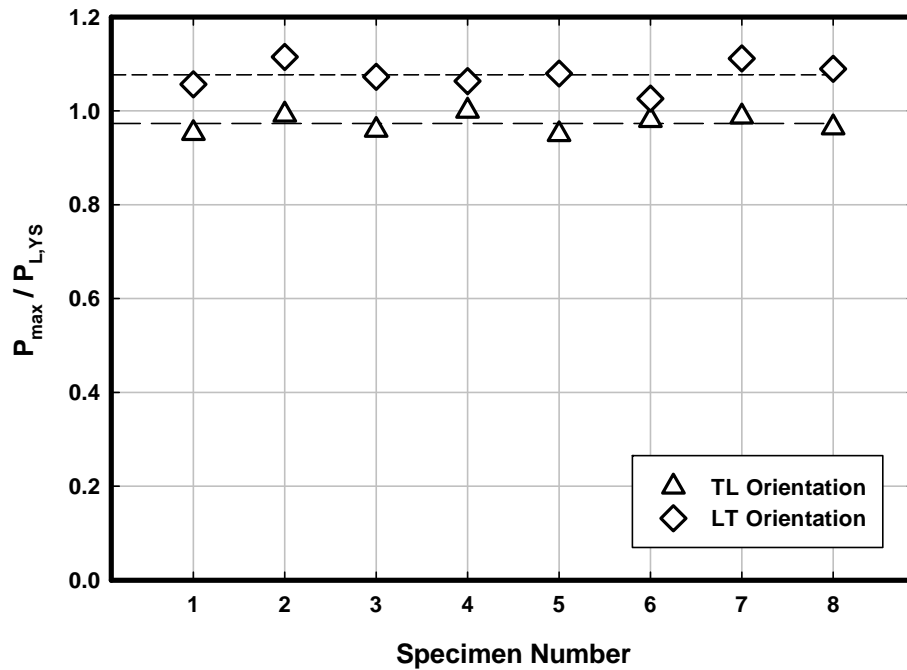


Figure 9 Ability of gusset plates to reach the yield strength-based limit load before fracture.

3.0) MEMBER TENSION TESTS

Tension tests were performed on a total of 72 locations from the five main truss members framing into the four U10 joints in the failed bridge. Each member consisted of either three or four individual plates welded together in either a box or H shape. One tension test specimen was cut from each plate in a given member. All tension test specimens were oriented in the longitudinal direction since the axial capacity of the members is of primary interest.

The specimens and ASTM testing procedures are identical to those outlined in the previous section for the gusset plate tests. All specimens are the 1.5 in. flat plate type cut from the full thickness of the plates according to the specimen geometry shown in Appendix A. Three different material grades were specified for the members in the design drawings as shown in Table 4. The specifications only list a maximum tensile strength requirement for grade 36 material.

Table 4 Strength and ductility requirements for structural steel in the ASTM A 709 Specifications.

Steel Grade	Minimum Yield Strength 0.2% Offset (ksi)	Minimum Tensile Strength (ksi)	Maximum Tensile Strength (MPa)	Minimum Elongation 8 in. (%)
36	36	58	80	20
50	50	65	n/a	18
50W	50	70	n/a	18

In addition to the main truss members, tension samples were tested from several of the rolled beams used to fabricate the floor truss members. For a given member three locations were tested, two in the flange and one in the web. Similar to the welded truss members, all specimens are machined in the longitudinal direction.

Results for the individual tension tests are listed in tables 5 through 9. The tables report the 0.2% offset yield strength (F_y), tensile strength (F_u), nominal thickness (t), percent elongation for a 8 in. gage length, and the reduction in area. Test results that fell below the specification strength by more than one percent are highlighted in yellow. In general, most of the results meet the specifications. The specification results are based on sampling either one location per plate or one location per heat of steel as specified in the design documents. It is not unusual to have test results that vary slightly at different locations. In addition, the test results are dependent on the rate of testing. The tests performed in this report are close to the slowest allowable rate while most specification tests are run close to the maximum rate. Therefore, the results in this report may be considered about 2 % conservative when making comparisons to specifications and mill reports. The fact that several individual test results fall slightly below the minimum required

strength should not be considered abnormal. The bridge design specifications account for material variability in the factor of safety.

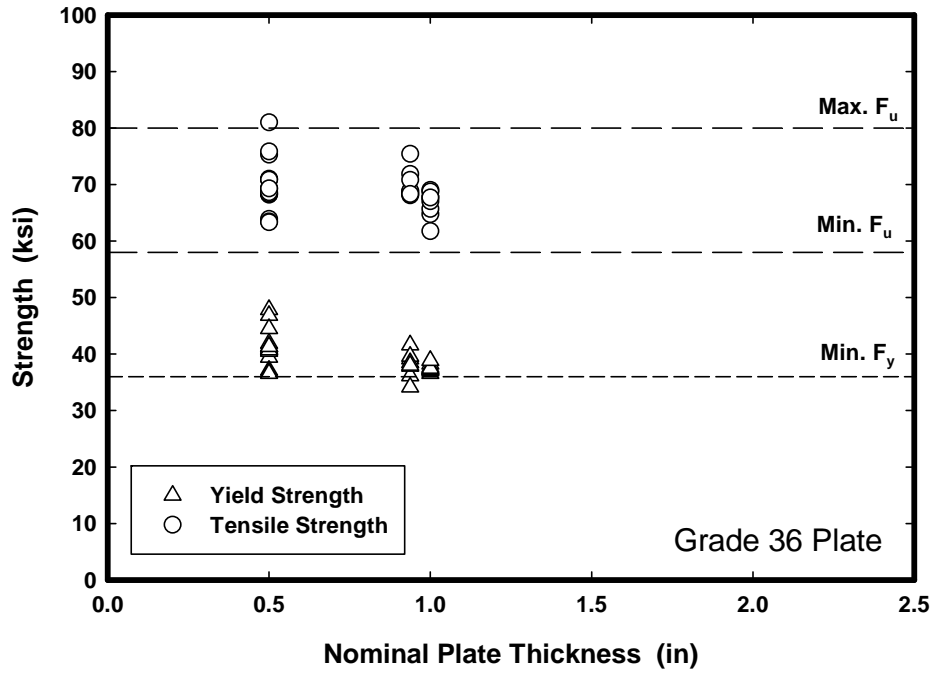


Figure 10 Tension test results for welded truss members fabricated from grade 36 steel plate.

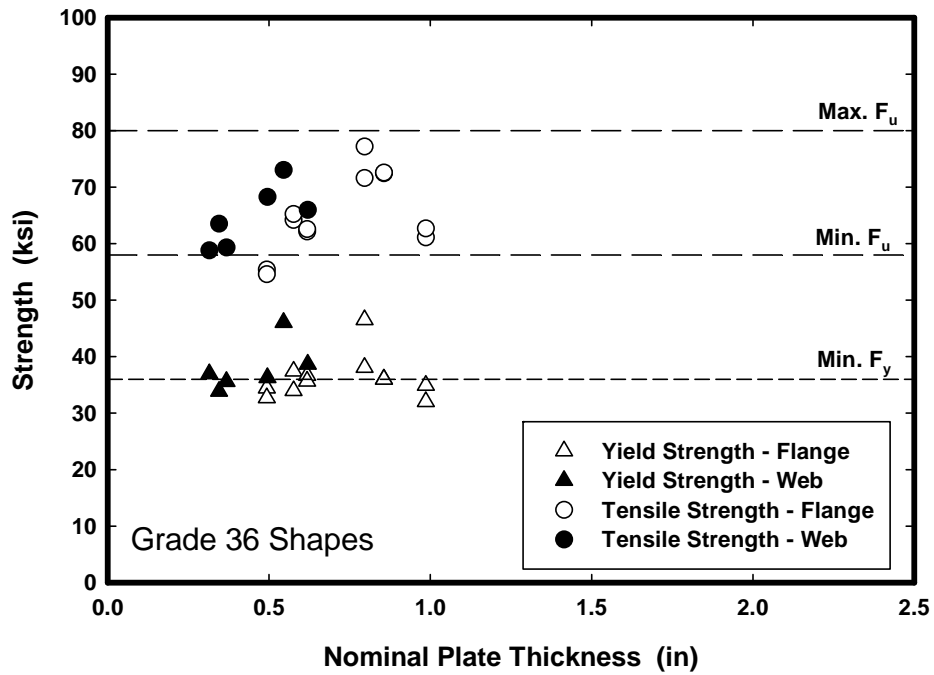


Figure 11 Tension test results for rolled shape members fabricated from grade 36 steel.

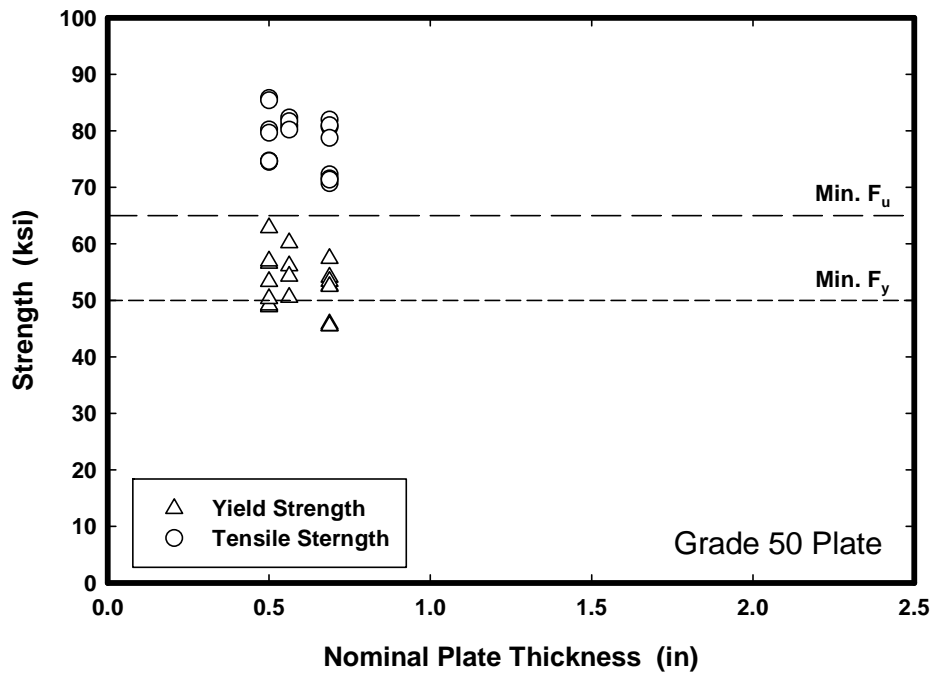


Figure 12 Tension test results for welded truss members fabricated from grade 50 steel plate.

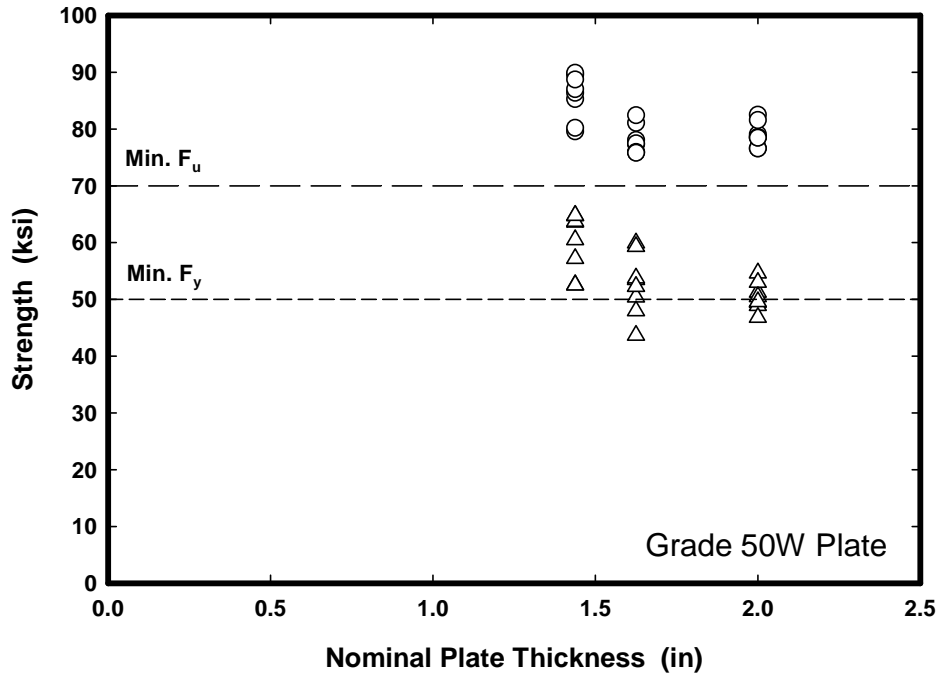


Figure 13 Tension test results for welded truss members fabricated from grade 50W steel plate.

Table 5 West Truss - South End - Main Members

MEMBER	PLATE	SPEC. ID	STEEL GRADE	t (in)	F _y (ksi)	F _u (ksi)	ELONG. 8 in. (%)	REDUCT. IN AREA (%)
U10-U12	Top	W41	36	0.5	36.00	70.81	25.4	51.0
	Bot.	W42	36	0.5	37.09	63.88	30.0	60.2
	East	W43	36	1.0	37.64	68.73	-	-
	West	W44	36	1.0	37.24	61.73	31.0	61.5
U8-U10	Top	W11	50	0.5	49.15	74.69	27.7	62.1
	Bot.	W12	50	0.5	53.32	80.20	23.4	60.1
	East	W13	50W	1.4375	63.72	89.87	22.9	54.2
	West	W14	50W	1.4375	64.79	88.70	26.0	60.0
L9-L11	Top	W71	36	0.5	40.44	69.17	27.4	51.8
	Bot.	W72	36	0.5	40.71	68.61	27.8	61.1
	East	W73	36	0.9375	39.58	68.86	29.7	64.1
	West	W74	36	0.9375	38.44	70.79	28.0	58.9
L9-U10	Top	W81	50	0.6875	54.11	81.96	22.1	60.6
	Bot.	W82	50	0.6875	53.37	80.97	24.3	60.1
	East	W83	50W	2.0	51.24	82.51	27.4	54.0
	West	W84	50W	2.0	52.99	81.56	28.5	58.1
U10-L11	Web	W33	50	0.5625	60.19	81.68	22.5	60.1
	East	W32	50W	1.625	53.76	77.45	27.7	60.4
	West	W31	50W	1.625	59.30	82.43	26.5	63.2

Table 6 West Truss - North End - Main Members

MEMBER	PLATE	SPEC. ID	STEEL GRADE	t (in)	F _y (ksi)	F _u (ksi)	ELONG. 8 in. (%)	REDUCT. IN AREA (%)
U10'-U12'	Top	W61	36	0.5	44.47	75.85	25.2	54.5
	Bot.	W62	36	0.5	36.78	63.43	27.0	58.8
	East	W63	36	1.0	37.43	67.02	24.6	61.0
	West	W64	36	1.0	38.83	67.66	29.3	62.7
U8'-U10'	Top	W21	50	0.5	50.29	74.62	24.8	55.2
	Bot.	W22	50	0.5	62.84	79.65	23.2	59.8
	East	W23	50W	1.4375	52.56	79.58	22.3	53.5
	West	W24	50W	1.4375	52.54	80.19	23.0	55.0
L9'-L11'	Top	W101	36	0.5	36.57	63.30	29.4	56.8
	Bot.	W102	36	0.5	41.30	69.30	27.0	58.4
	East	W103	36	0.9375	34.13	68.31	27.3	61.7
	West	W104	36	0.9375	38.00	75.43	29.8	64.0
L9'-U10'	Top	W91	50	0.6875	45.49	71.33	25.9	58.4
	Bot.	W92	50	0.6875	52.44	78.74	26.5	58.8
	East	W93	50W	2.0	50.46	78.51	29.8	57.0
	West	W94	50W	2.0	49.58	78.43	27.1	55.0
U10-L11	Web	W53	50	0.5625	50.54	80.19	21.8	61.1
	East	W52	50W	1.6250	52.27	75.79	27.4	61.2
	West	W51	50W	1.6250	43.68	75.94	28.3	61.4

Table 7 East Truss - South End - Main Members

MEMBER	PLATE	SPEC. ID	STEEL GRADE	t (in)	F _y (ksi)	F _u (ksi)	ELONG. 8 in. (%)	REDUCT. IN AREA (%)
U10-U12	Top	E31	36	0.5	47.85	80.97	22.4	48.0
	Bottom	E32	36	0.5	41.88	70.98	26.7	56.6
	East	E33	36	1.0	36.54	67.73	28.8	58.1
	West	E34	36	1.0	37.01	64.73	29.8	60.7
U8-U10	Top	E11	50	0.5	49.10	74.57	22.6	53.1
	Bottom	E12	50	0.5	56.57	85.77	19.3	55.5
	East	E13	50W	1.4375	63.57	89.55	22.8	52.9
	West	E14	50W	1.4375	64.72	85.26	23.3	62.2
L9-L11	Top	E71	36	0.5	41.29	70.81	25.0	56.3
	Bottom	E72	36	0.5	40.71	69.34	26.9	51.4
	East	E73	36	0.9375	41.58	68.70	-	-
	West	E74	36	0.9375	39.12	68.07	29.3	61.9
L9-U10	Top	E61	50	0.6875	52.60	80.66	24.9	61.8
	Bottom	E62	50	0.6875	57.41	72.27	20.3	48.4
	East	E63	50W	2.0	54.65	79.05	26.6	59.2
	West	E64	50W	2.0	49.48	78.57	29.5	59.4
U10-L11	Web	E103	50	0.5625	54.28	82.32	20.4	55.9
	East	E102	50W	1.6250	47.98	77.31	28.5	65.2
	West	E101	50W	1.6250	59.93	81.08	26.5	62.6

Table 8 East Truss - North End - Main Members

MEMBER	PLATE	SPEC. ID	STEEL GRADE	t (in)	F _y (ksi)	F _u (ksi)	ELONG. 8 in. (%)	REDUCT. IN AREA (%)
U10'-U12'	Top	E51	36	0.5	46.82	75.27	22.5	52.2
	Bottom	E52	36	0.5	41.00	68.19	28.0	57.9
	East	E53	36	1.0	37.28	69.02	26.8	62.8
	West	E54	36	1.0	38.21	65.66	30.3	63.6
U8'-U10'	Top	E21	50	0.5	48.86	74.49	23.8	61.9
	Bottom	E22	50	0.5	56.95	85.38	21.0	56.5
	East	E23	50W	1.4375	57.18	86.36	22.3	53.5
	West	E24	50W	1.4375	60.51	87.01	23.0	55.0
L9'-L11'	Top	E91	36	0.5	39.41	68.28	25.9	53.7
	Bottom	E92	36	0.5	41.26	68.38	25.9	57.2
	East	E93	36	0.9375	36.13	68.31	26.8	64.3
	West	E94	36	0.9375	37.82	71.84	28.8	64.0
L9'-U10'	Top	E81	50	0.6875	45.81	71.53	25.9	62.9
	Bottom	E82	50	0.6875	45.47	70.69	27.2	61.7
	East	E83	50W	2.0	51.24	82.51	30.2	59.6
	West	E84	50W	2.0	52.99	81.56	32.9	58.3
U10-L11	Web	E43	50	0.5625	56.09	80.84	22.2	58.4
	East	E42	50W	1.625	53.47	78.03	26.6	59.8
	West	E41	50W	1.625	50.41	75.88	28.6	64.1

Table 9 Floor Truss 10 Members

MEMBER	PLATE	SPEC. ID	STEEL GRADE	t (in)	F _y (ksi)	F _u (ksi)	ELONG. 8 in. (%)	REDUCT. IN AREA (%)
U13-U14	Top	F11	36	0.576	33.95	64.16	28.0	52.9
	Bottom	F12	36	0.576	37.41	65.22	26.3	55.1
	Web	F13	36	0.345	33.84	63.51	24.4	51.9
U4-L4	Top	F21	36	0.493	34.43	55.38	31.6	57.8
	Bottom	F22	36	0.493	32.71	54.56	33.8	60.9
	Web	F23	36	0.315	36.96	58.79	20.5	48.9
U3-L4	Top	F31	36	0.618	36.67	62.12	29.5	57.5
	Bottom	F32	36	0.618	35.65	62.55	28.9	57.2
	Web	F33	36	0.368	35.58	59.30	31.6	57.8
L2-L4	Top	F51	36	0.796	46.53	77.16	27.4	49.9
	Bottom	F52	36	0.796	38.08	71.58	27.7	56.5
	Web	F53	36	0.495	36.27	68.25	26.0	57.3
L2-U3	Top	F61	36	0.856	36.02	72.46	28.0	52.0
	Bottom	F62	36	0.856	36.00	72.56	25.0	55.0
	Web	F63	36	0.545	46.05	73.03	18.6	49.3

Figure 10 shows the results for all of the grade 36 structural plate with the yield and tensile strengths plotted versus plate thickness. It is normal to see a trend toward somewhat higher strength for thinner plates for a given grade. The plot shows that one test result exceeded the maximum tensile stress and several results were slightly below the minimum specified yield strength. These results can be considered typical and do not indicate deficient material.

The results for the grade 36 rolled beams shown in figure 11 show several test results falling below the minimum requirements for both yield and tensile strength. In general, rolled shapes typically have larger variability in strength related to sample location than structural plate. The flanges and webs in rolled shaped undergo different amounts of area reduction during the steel making process that leads to increased variability compared to plate. Therefore, the rolled shape results can be considered typical.

Figures 12 and 13 show the results for the grade 50 and 50W plate material. It appears that grade 50W was specified for the thicker plates while grade 50 was used in the thinner plates at this strength level. The main difference between the two grades is that the 50W grade has enhanced corrosion resistance and is suitable for use without paint. Since the I-35W truss is a painted bridge, it is doubtful that atmospheric corrosion resistance was a factor in material selection. Since the added alloy content of the 50W grade typically produces plate with higher CVN toughness, this may have been the reason it was specified for the thicker plates. Based on yield strength, both grades can be considered structurally equivalent. Similar to the grade 36 plate results, there are several individual tests that fall below the specified minimum yield strength. However, for the aforementioned reasons, this can be considered typical material.

4.0) DECK AND PIER CONCRETE CORE TESTS

Compressive strength, compressive modulus of elasticity, and coefficient of thermal expansion tests were completed on select concrete cores obtained from the bridge deck and the piers of the collapsed I-35W bridge in Minneapolis. These cores were obtained from sections of the collapsed deck and from Piers 5 through 8 by Wiss Janney Elstner (WJE) personnel. Locations of the cores will be summarized in a separate WJE report. The tests were conducted during October and November 2007 at the FHWA Turner-Fairbank Highway Research Center.

Table 10 provides the results of these tests. Except where noted, compression modulus of elasticity tests were conducted according to ASTM C 469, compressive strength tests were conducted according to ASTM C 39, and coefficient of thermal expansion tests were conducted according to AASHTO TP-60.

The cores were obtained by drilling a core bit into the face of the concrete structure. In the case of the deck, the cores were drilled from above through the entire depth of the deck, including both the structural deck as well as any concrete overlay that was on the deck at the location cored. These cores inevitably contained reinforcing steel which was encountered during the drilling. In the case of the piers, the cores were obtained by drilling laterally into the side of the pier columns within 5 feet of ground level. The pier column core drilling passed through the reinforcing steel cage into the center of the column so as to obtain a reinforcing steel-free core.

The density values presented in Table 10 are indicative of the density of the concrete in the deck and piers, exclusive of any included reinforcing bar. These values were calculated using the volume of the each core prior to testing, the weight of each core prior to testing, and the weight and volume of any included reinforcing steel. Pieces of reinforcing bar were contained in each deck core; these pieces were extracted from the cores and measured after the conclusion of all other testing.

The average density of the pier concrete is 149 lb/ft³. The average density of the deck concrete cores is 148 lb/ft³. However, the deck concrete cores were composed of varying proportions of structural and overlay concretes with different mix designs and different densities. For this reason, additional density calculations were completed on the deck overlay at core locations 6K and 6L. Approximately 1 in. thick by 3.75" diameter core slices were tested according to the ASTM C127 test methodology. These tests indicated that the overlay concrete, exclusive of air voids, has a density of approximately 144.7 lb/ft³. Assuming an air void content of 3%, the density of the overlay concrete is 140 lb/ft³. Based on this value and the proportions of overlay to structural concrete in the five deck cores, the density of the structural deck concrete was determined to be approximately 150 lb/ft³.

In order to complete the ASTM C 469 modulus of elasticity test, the concrete compressive strength must first be approximated. One deck core (Deck 6F) and one pier core (Pier 5 West #1) were tested according to ASTM C 39 to determine the compressive strength.

Based on these results, the load levels for ASTM C 469 were determined and this test was completed for 8 other pier cores and 2 other deck cores. Subsequently, all 10 of these cores were tested for compressive strength according to ASTM C 39. Note that completing ASTM C 39 after ASTM C 469 is considered acceptable as long as the upper load level reached during the ASTM C 469 test is less than or equal to 40% of the compressive strength.

The average modulus of elasticity from the seven pier cores tested according to the specification is 5330 ksi with a standard deviation of 300 ksi. The average of the two deck cores is 4820 ksi. The average compressive strength of the nine pier cores tested according to the specification is 9.7 ksi with a standard deviation of 1.0 ksi. The average of the two deck cores tested according to the specification is 8.3 ksi.

The coefficient of thermal expansion tests were completed according to AASHTO TP-60. The cores were soaked in a lime-water bath for 4 weeks prior to the initiation of testing. Each core was tested twice, once in each of two independent testing machines, and the average result is reported. Based on the two cores tested, the average coefficient of thermal expansion of the deck concrete is 5.3×10^{-6} in/in/°F.

Table 10 Concrete core mechanical property results.

CORE [†]	DIAMETER (in.)	LENGTH (in.)	DENSITY [‡] (lb/ft ³)	MODULUS OF ELASTICITY (ksi)	COMPRESSIVE STRENGTH (ksi)	COEFF. OF EXPANSION (in/in/°F)
Pier 5 West #1	3.77	7.47	148.4	---	11.0	---
Pier 5 West #2	3.77	7.51	148.7	5630	8.0	---
Pier 5 East #4	3.73	7.44	147.7	5050	9.3	---
Pier 6 West #3	3.74	7.44	150.3	5010	9.4	---
Pier 6 West #4	3.75	7.70	149.8	5100	9.6	---
Pier 6 East #5	3.76	7.50	150.4	5380	11.1	---
Pier 7 West #3	3.69	7.82	147.4	5370	9.8	---
Pier 8 East #5	3.77	7.43	151.4	5790	9.4	---
Pier 8 East #10	3.76	7.74	149.5	5540 ^a	7.0 ^a	---
Deck 6F	3.72	5.63 ^c	150.4	---	7.5 ^b	---
Deck 6K	3.75	7.53 ^d	149.0	4610 ^h	7.4	---
Deck 9A	3.72	7.56 ^e	146.0	5040 ⁱ	9.2	---
Deck 6L	3.75	7.04 ^f	150.9	---	---	5.2 x 10 ⁻⁶
Deck 9B	3.72	7.14 ^g	144.2	---	---	5.3 x 10 ⁻⁶

† Six other cores were not suitable for testing due to fractures, chips, or large included rebar: Pier 5 East #3, Pier 6 West #1, Pier 6 West #2, Pier 8 West #1, Deck 8M, and Deck 6P.

‡ Density calculations are exclusive of rebar contained within core

a Loaded to 51% of compressive strength during Modulus of Elasticity test

b Under-length (Length/Diameter = 1.51)

c No overlay

d 18% of core is overlay

e 30% of core is overlay

f 14% of core length is overlay

g 51% of core length is overlay

h 95% deck concrete, 5% overlay concrete within compressometer gage length

i 80% deck concrete, 20% overlay concrete within compressometer gage length

REFERENCES

ASTM A 441 (Discontinued - replaced by ASTM A572)

ASTM E 8-08 *Standard Test Methods for Tension Testing of Metallic Materials.*

ASTM E 23-07a *Standard Test Methods for Notched Bar Impact Testing of Metallic Materials.*

ASTM A 673-07 *Standard Specification for Sampling Procedure for Impact Testing of Structural Steel.*

ASTM A 709-07 *Standard Specification for Structural Steel for Bridges.*

ASTM E 1820-08 *Standard Test Method for Measurement of Fracture Toughness.*

ASTM C 469-02E1 *Standard Test Method for Static Modulus of Elasticity and Poisson's Ratio of Concrete in Compression.*

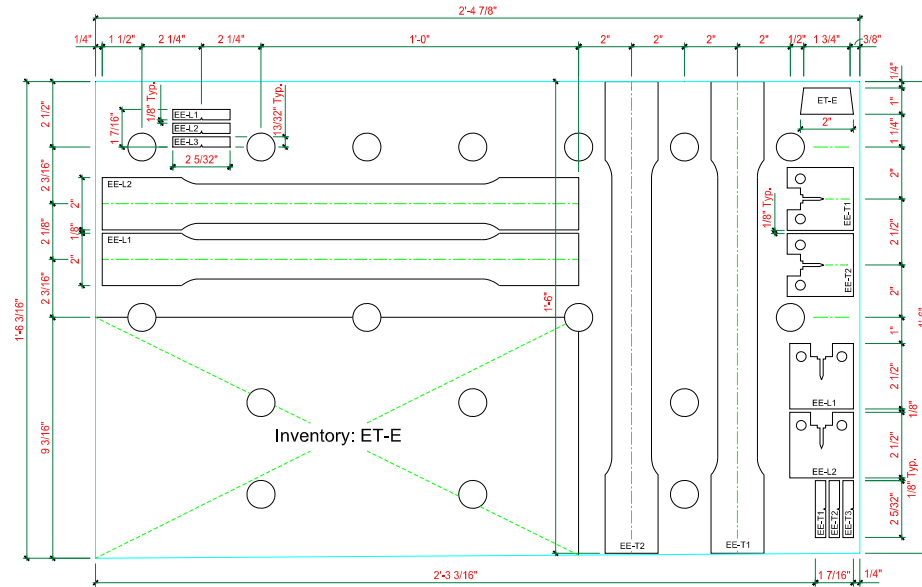
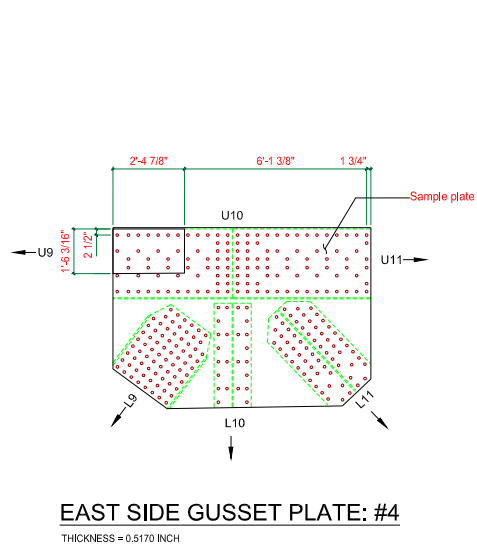
ASTM C 39-05E1 *Standard Test Method for Compressive Strength of Cylindrical Concrete Specimens.*

AASHTO TP 60 *Standard Method of Test for Coefficient of thermal Expansion of Hydraulic Cement Concrete.*

Wright, W. J., Candra, H., and Albrecht, P.,(2006) *Limit Load Analysis for Fracture Prediction in High-Performance Steel Bridge Members*, Journal of Bridge Structures: Assessment, Design, and Construction, Vol. 2, Dec.

Appendix A

Specimen Marking and Cut Plan for the U-10 Gusset Plates



SPECIMEN LAYOUT

- NOTE:
 1. EE = EAST TRUSS- EAST SIDE GUSSET PLATE
 2. L = LONGITUDINAL, PARALLEL TO ROLLING
 3. T = TRANSVERSAL, PERPENDICULAR TO ROLLING

Figure A1 Location of Specimens on U10 East Truss, East Side Gusset Plate.

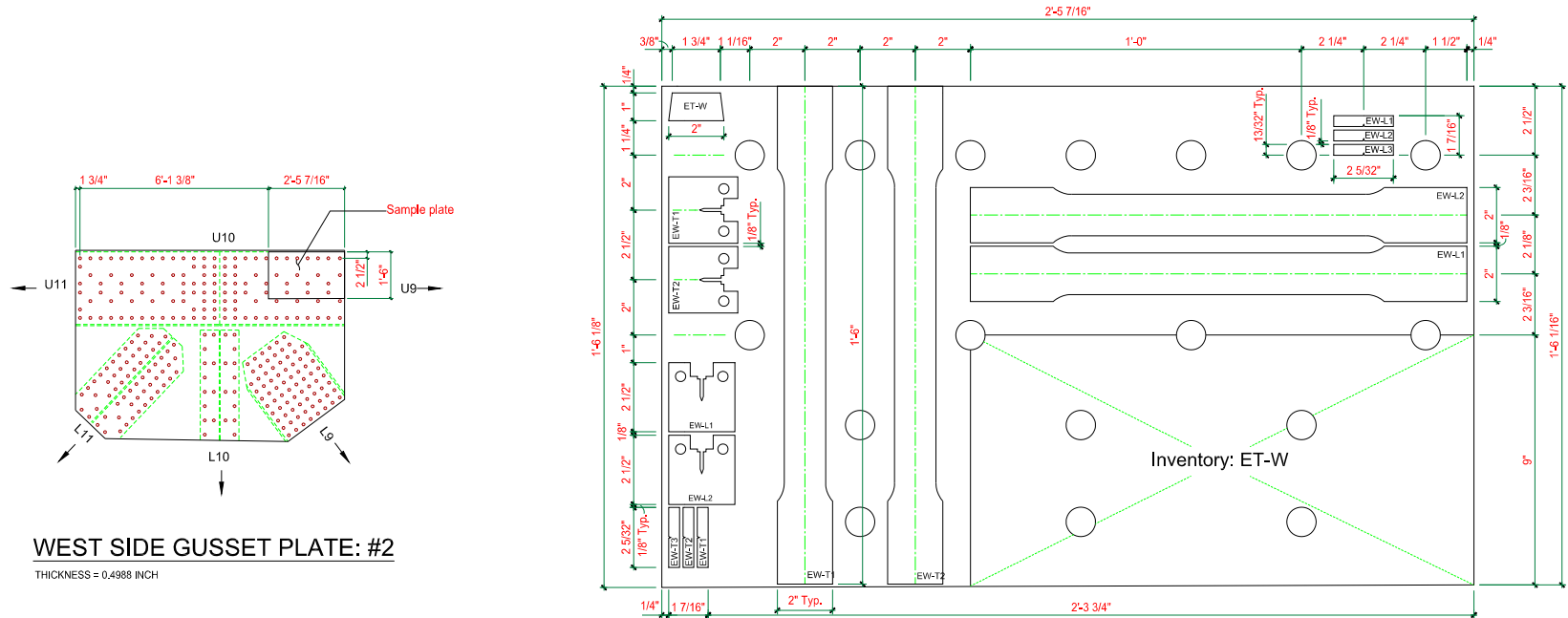
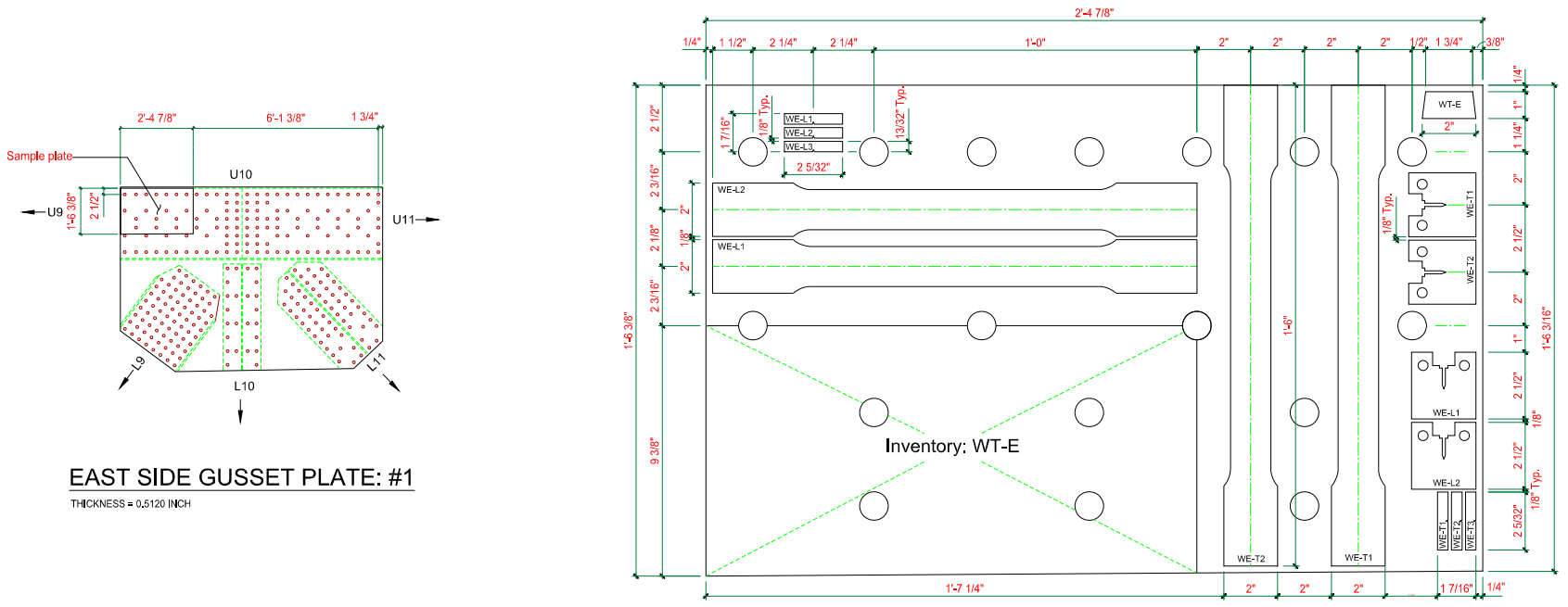


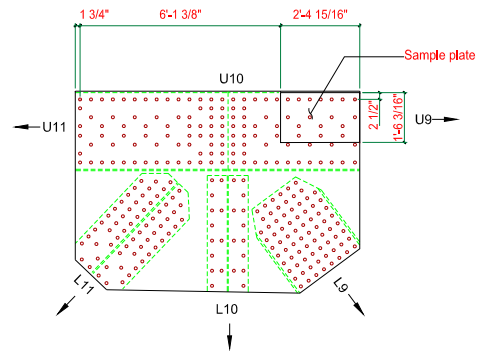
Figure A2 Location of Specimens on U10 East Truss, West Side Gusset Plate.



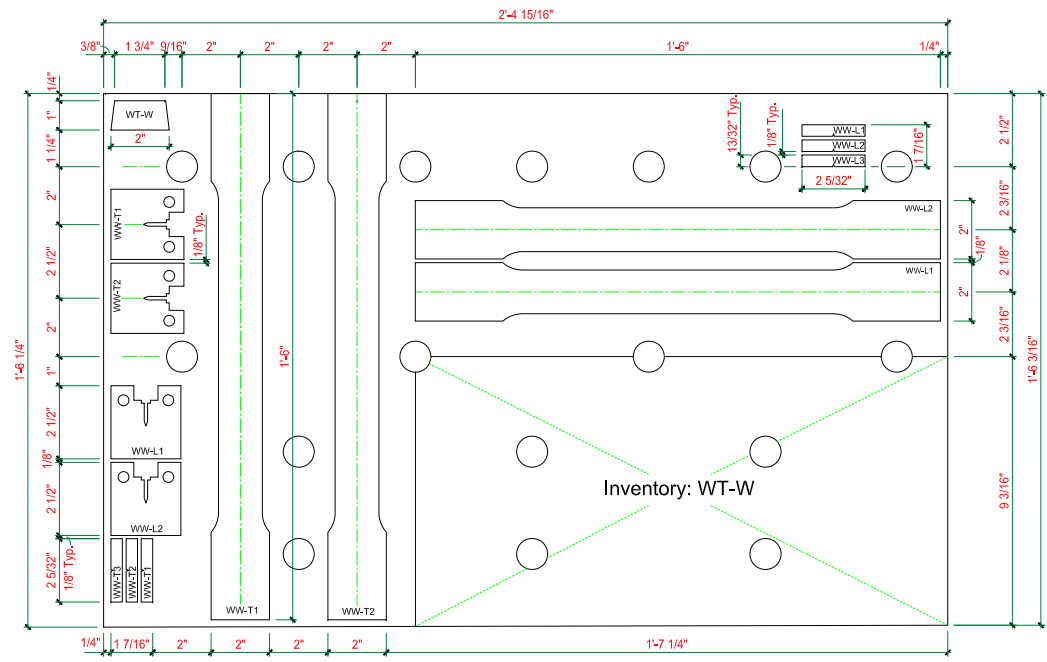
SPECIMEN LAYOUT

- NOTE:
 1. WE = WEST TRUSS- EAST SIDE GUSSET PLATE
 2. L = LONGITUDINAL, PARALLEL TO ROLLING
 3. T = TRANSVERSAL, PERPENDICULAR TO ROLLING

Figure A 3 Location of Specimens on U10 West Truss, East Gusset Plate.



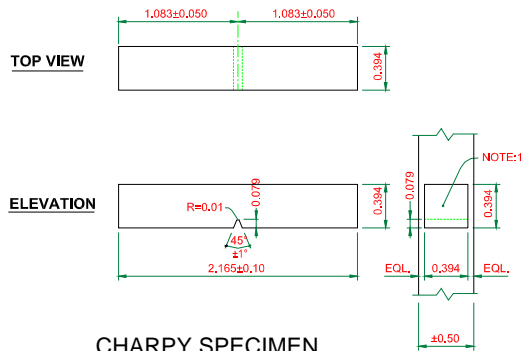
WEST SIDE GUSSET PLATE: #3
 THICKNESS = 0.5050 INCH



SPECIMEN LAYOUT

- NOTE:
1. WW = WEST TRUSS- WEST SIDE GUSSET PLATE
 2. L = LONGITUDINAL, PARALLEL TO ROLLING
 3. T = TRANSVERSAL, PERPENDICULAR TO ROLLING

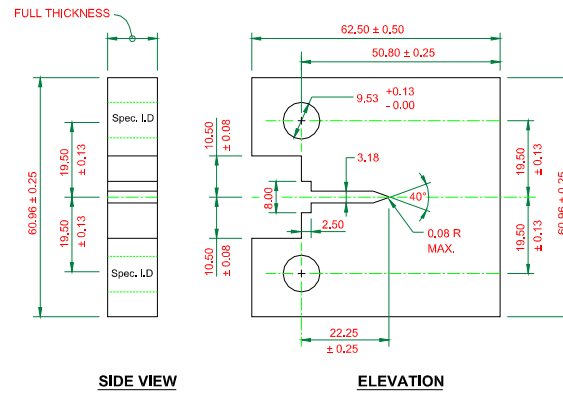
Figure A 4 Location of Specimens on U10 West Truss, West Gusset Plate.



CHARPY SPECIMEN

NOTES:

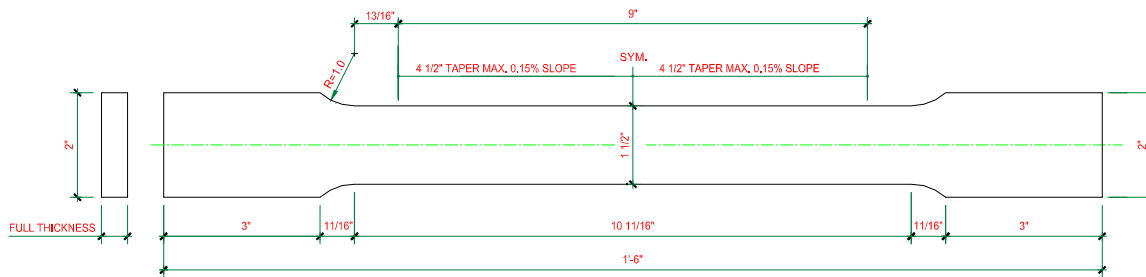
1. STAMP SPECIMEN IDENTIFICATION AT BOTH END (SEE LAYOUT DRAWING FOR SPEC. I.D.)
2. ALLOWABLE DIMENSIONAL TOLERANCE = ± 0.1
3. ALL DIMENSIONS ARE SHOWN IN MM



C(T) SPECIMEN

NOTES:

1. STAMP SPECIMEN IDENTIFICATION AT BOTH END (SEE LAYOUT DRAWING FOR SPEC. I.D.)
2. ALL DIMENSIONS ARE SHOWN IN MM



TENSION SPECIMEN

NOTES:

1. STAMP SPECIMEN IDENTIFICATION AT BOTH END (SEE LAYOUT DRAWING FOR SPEC. I.D.)
2. ALL DIMENSIONS ARE SHOWN IN INCH

Figure A5 Tension, Charpy and C(T) Specimens

Appendix B

Stress - Strain Curves for the U-10 Gusset Plate Tension Tests.

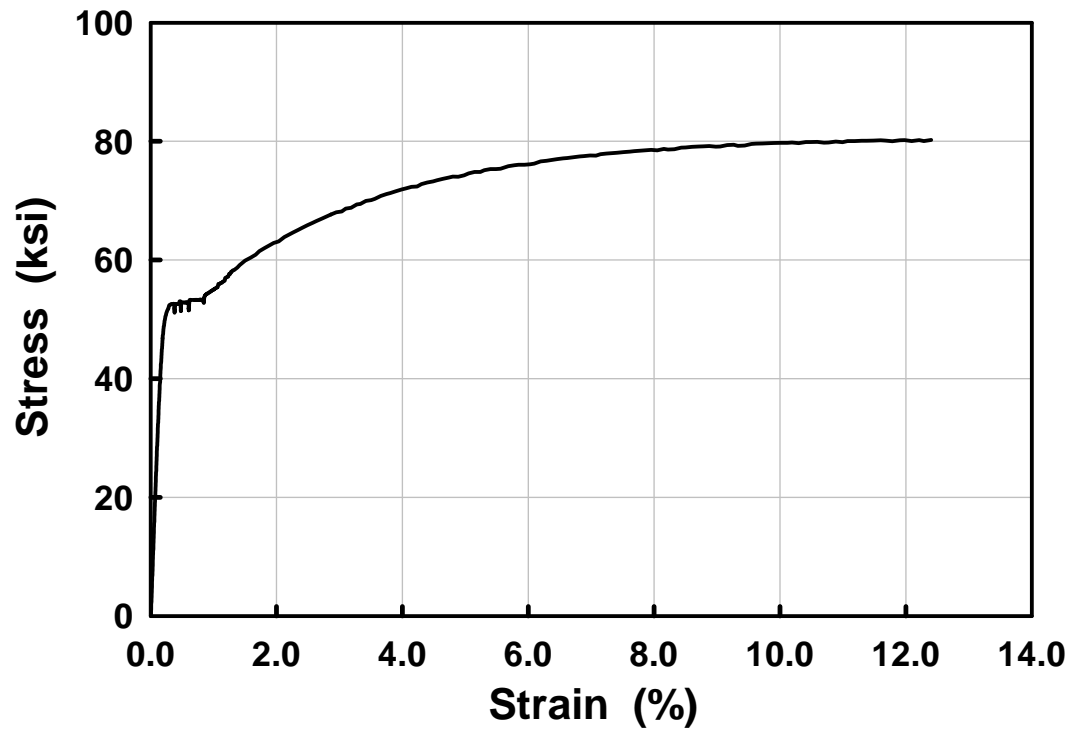


Figure B1 Stress-Strain Curve for Specimen WE-L1.

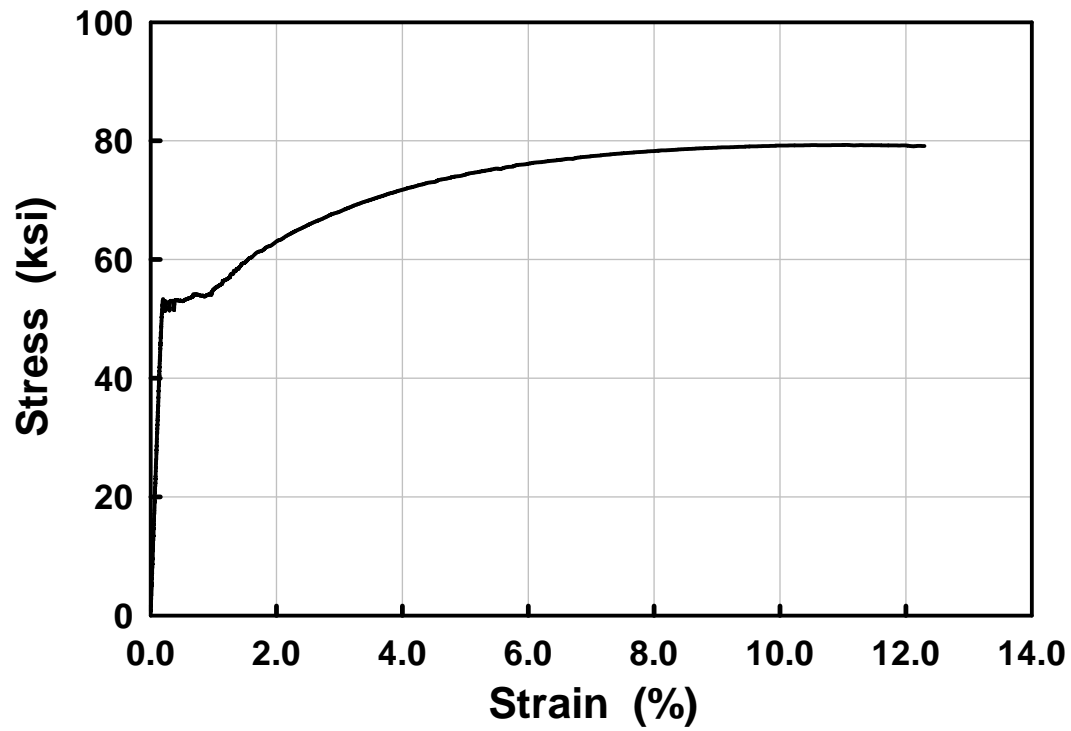


Figure B2 Stress-strain Curve for Specimen WE-L2.

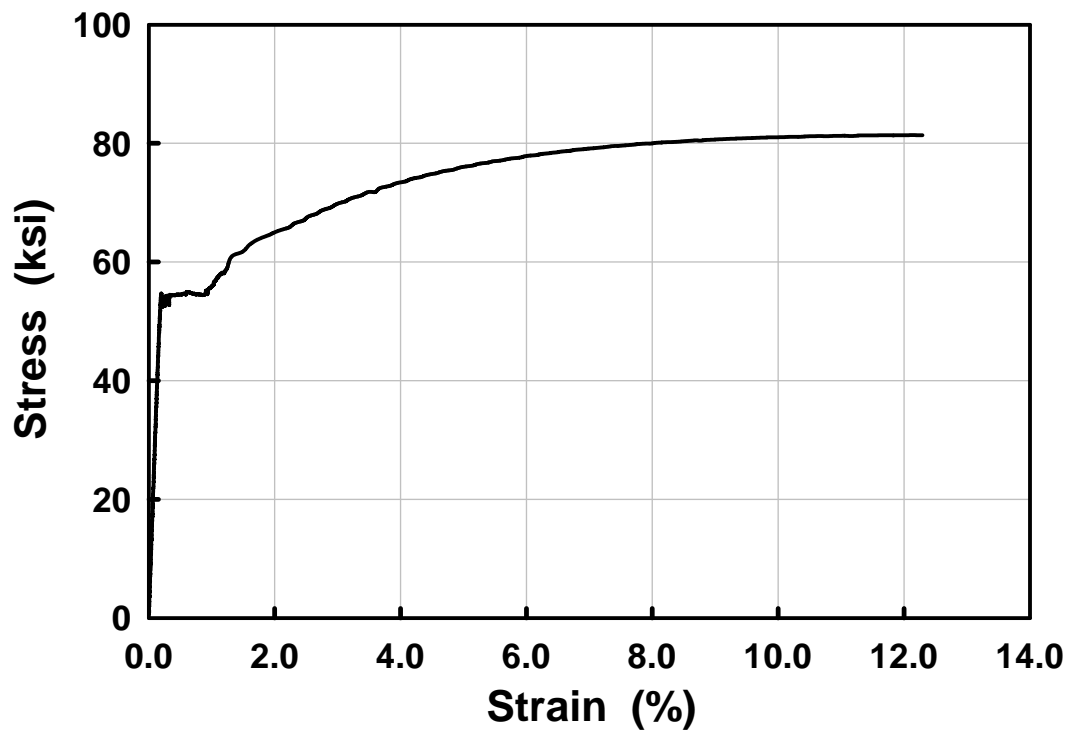


Figure B3 Stress-Strain Curve for Specimen WE-T1.

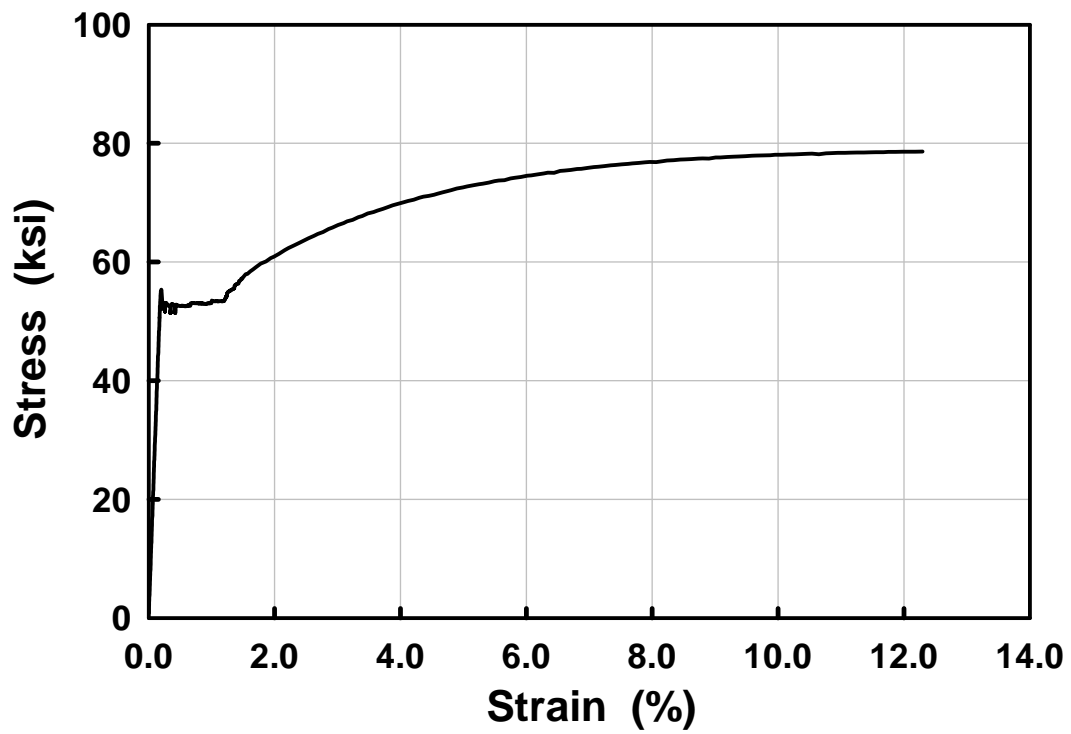


Figure B4 Stress-Strain Curve for Specimen WW-L1.

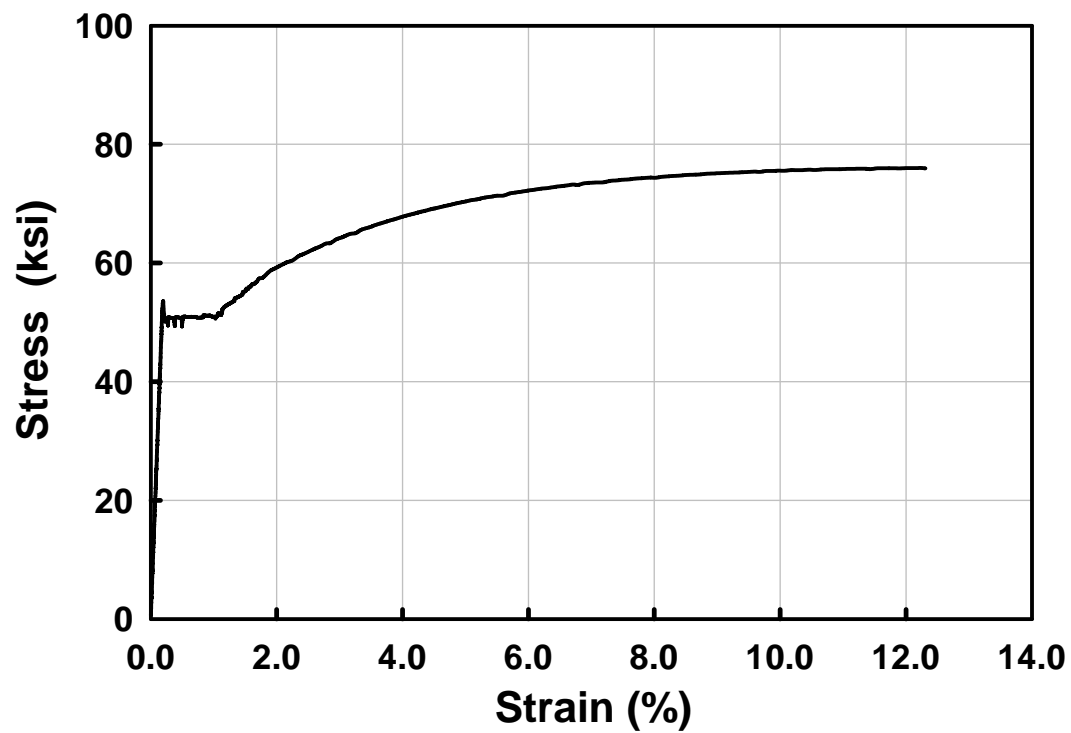


Figure B5 Stress-Strain Curve for Specimen WW-L2.

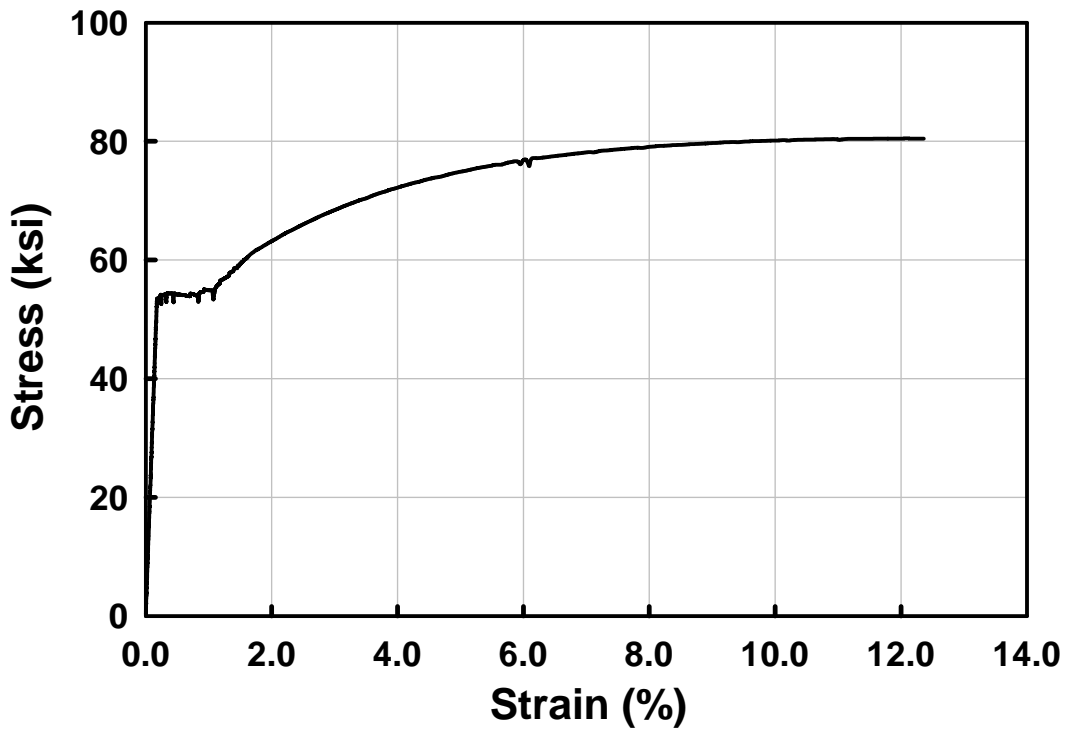


Figure B6 Stress-Strain Curve for Specimen WW-T1.

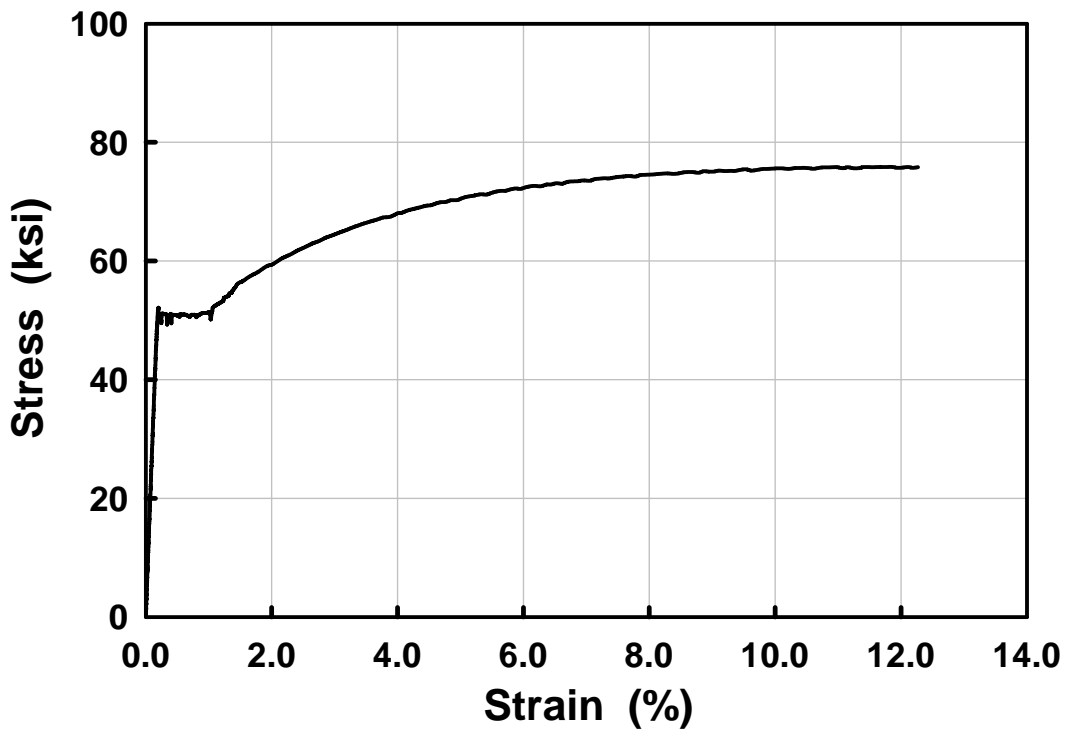


Figure B7 Stress-Strain Curve for Specimen WW-T2.

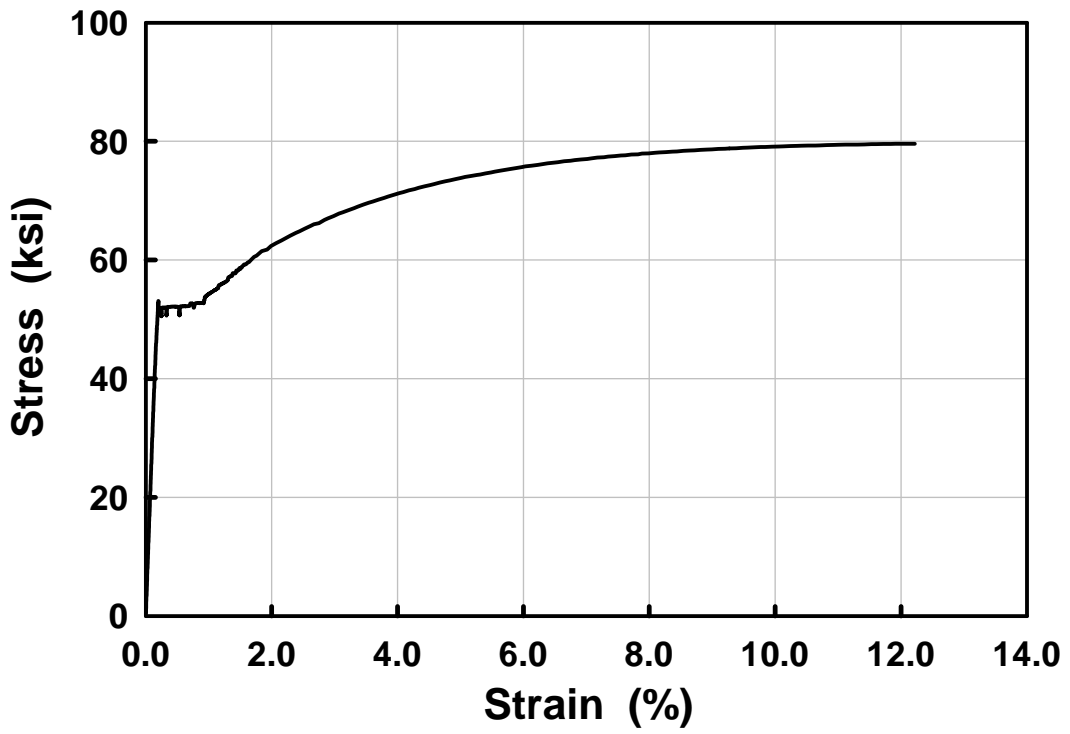


Figure B8 Stress-Strain Curve for Specimen EW-L1.

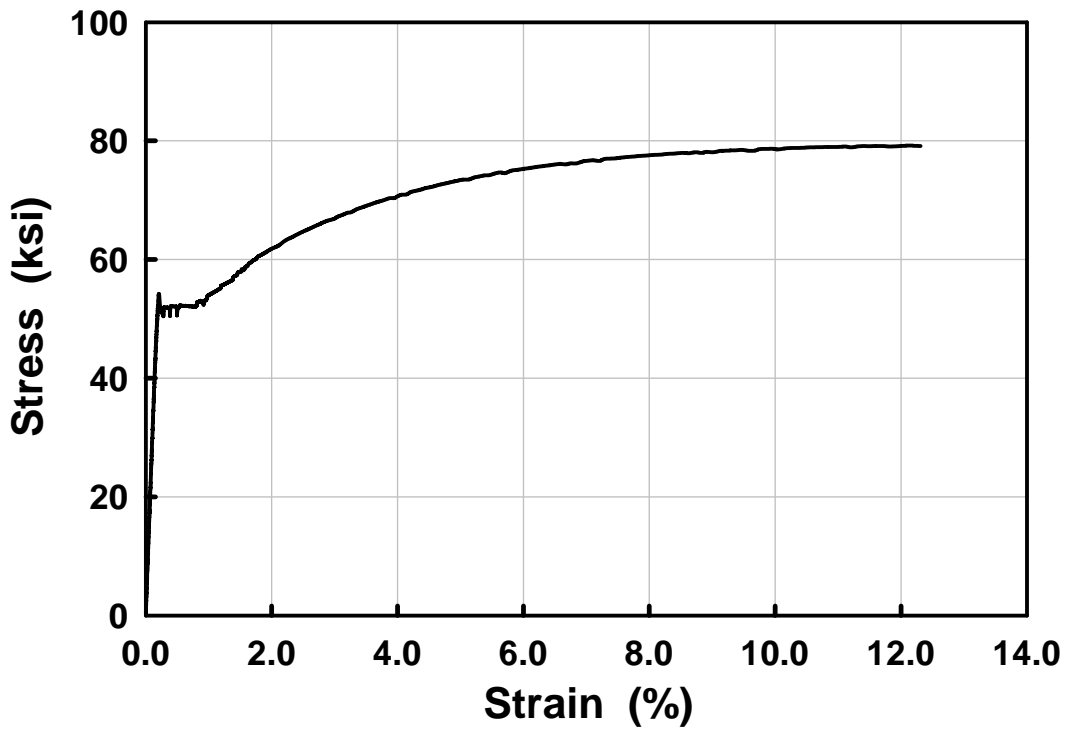


Figure B9 Stress-Strain Curve for Specimen EW-L2.

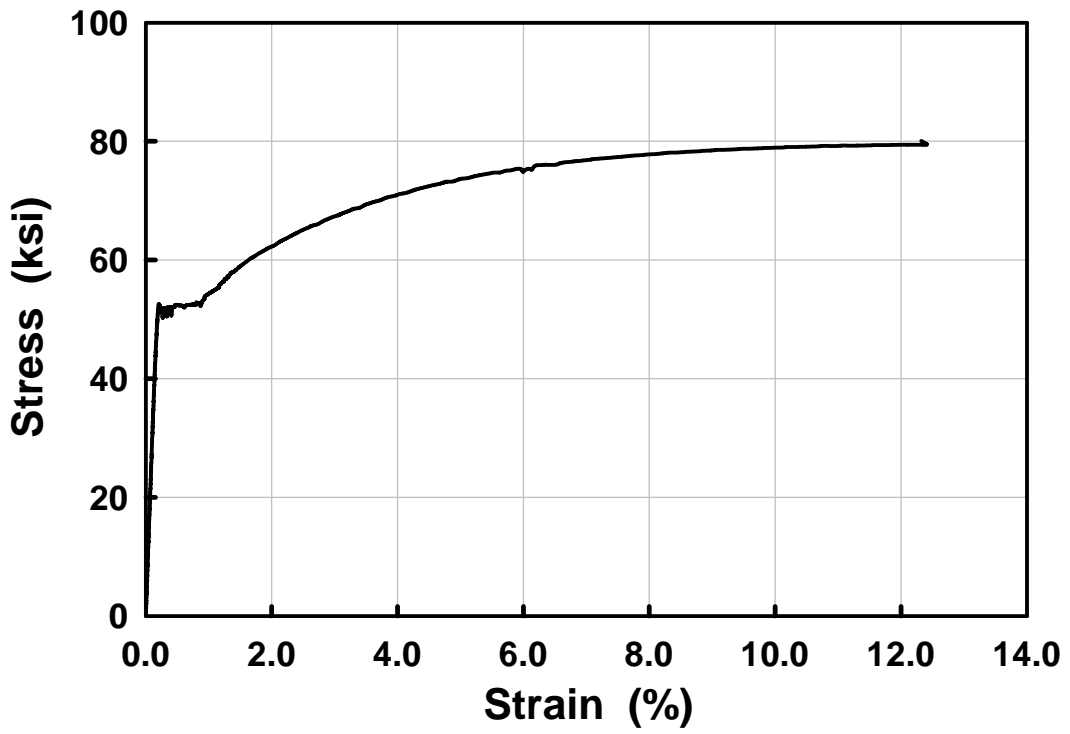


Figure B10 Stress-Strain Curve for Specimen EW-T1.

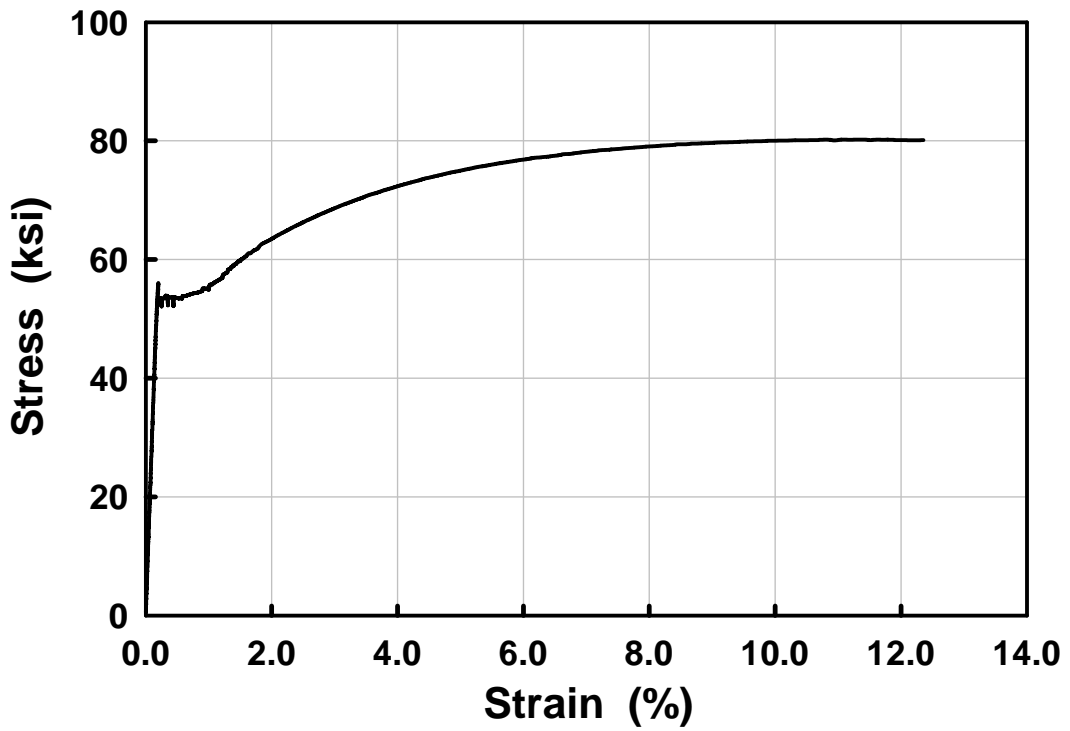


Figure B11 Stress-Strain Curve for Specimen EW-T2.

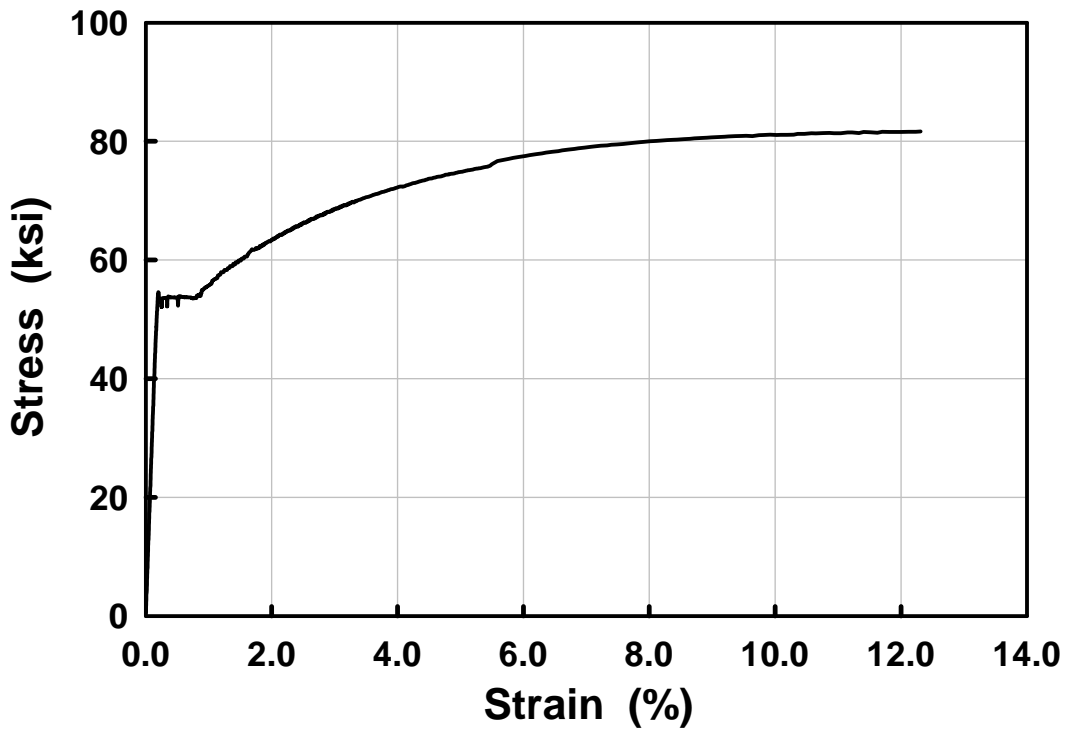


Figure B12 Stress-Strain Curve for Specimen EE-L1.

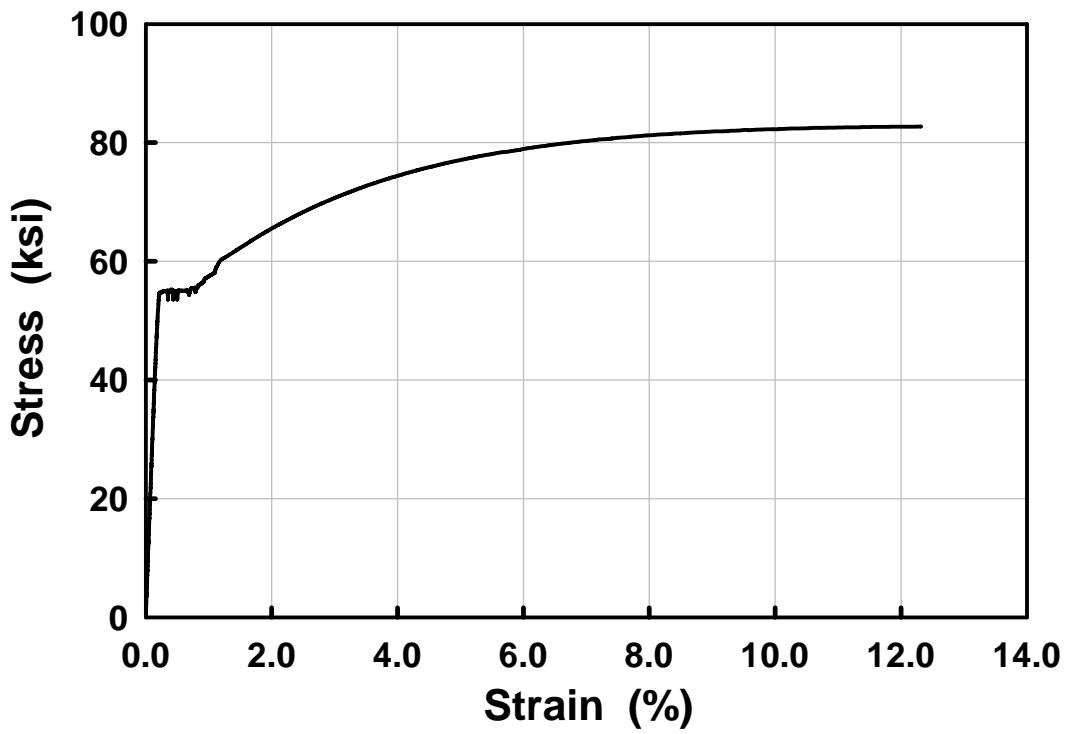


Figure B13 Stress-Strain Curve for Specimen EE-L2.

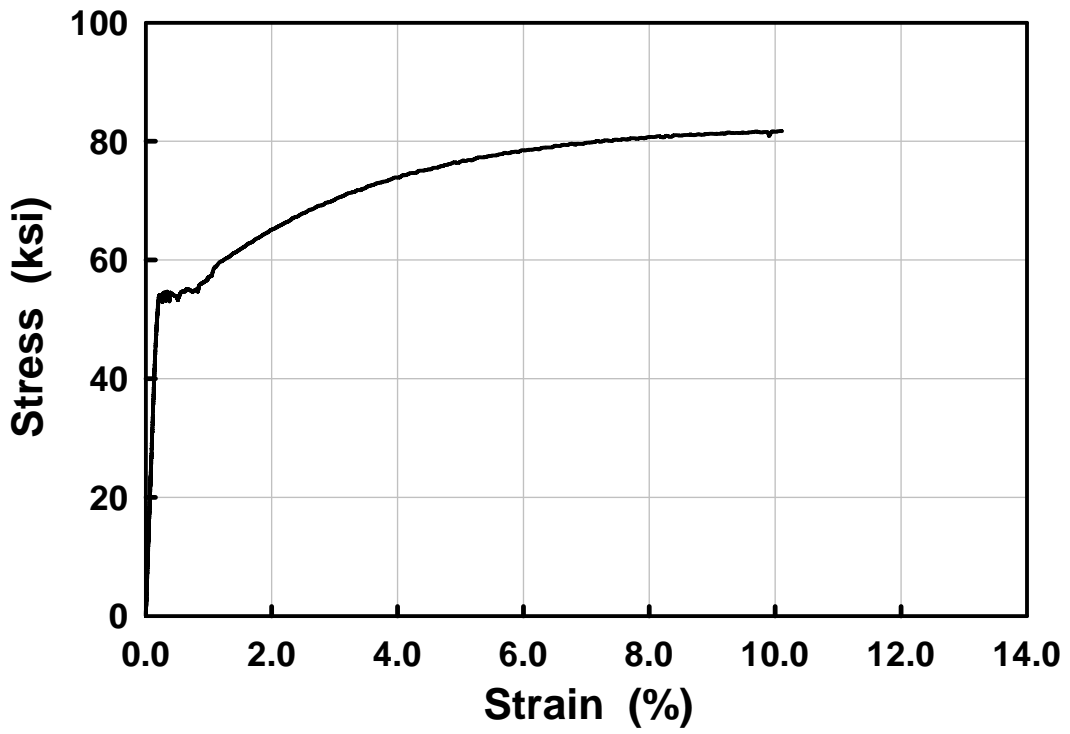


Figure B14 Stress-Strain Curve for Specimen EE-T1.

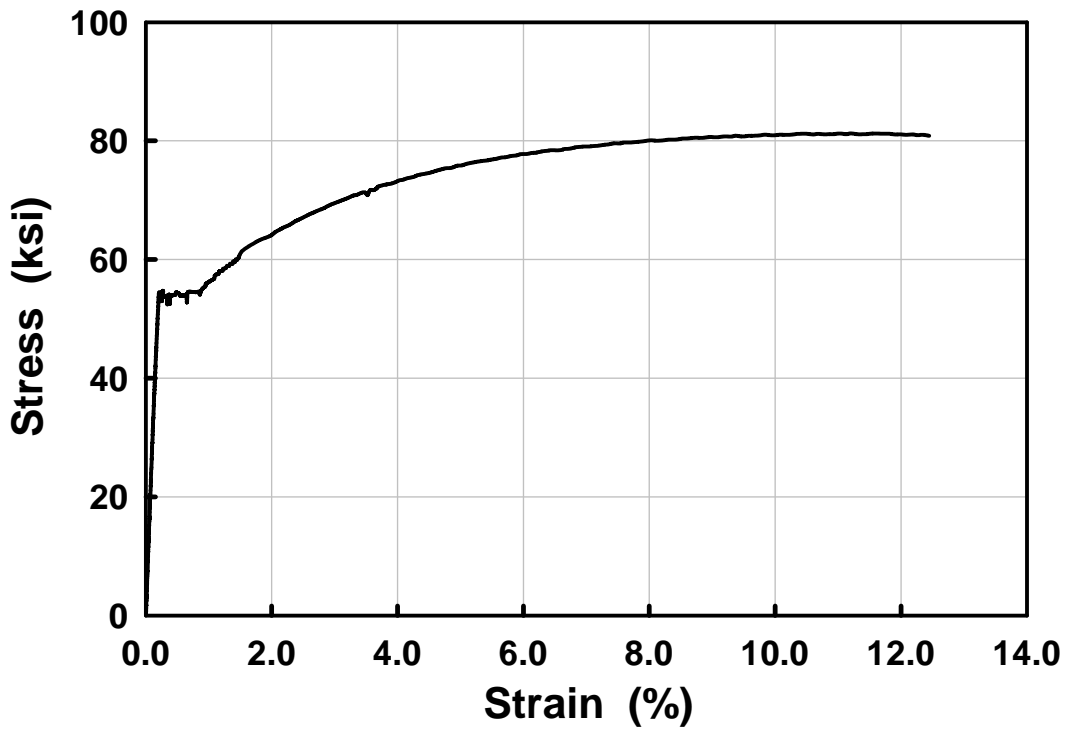


Figure B15 Stress-Strain Curve for Specimen EE-T2.

Appendix C

Compact Tension Test Results for the U-10 Gusset Plates

Terminology

Definition of Terms For Fracture Test (Table C1)

a_0	Initial measured crack length
a_{0q}	Initial predicted crack length
a_f	Final measured crack length
Δa_p	Measured crack extension
$\Delta a_{\text{predicted}}$	Predicted crack extension
B	Specimen thickness
B_N	Side groove thickness
W	Specimen size
a_N	Machined notch length
H	Specimen size

List of Terms For Precracking (Table C2)

a_{initial}	Initial predicted crack length
a_{final}	Final predicted crack length
Slope Correlation	Fit quality for crack length prediction
ΔK	Stress intensity factor range
R-ratio	Load ratio
N	Number of cycles

Figures

v_g	Load line displacement measured with a clip gage
P	Force on the specimen through the pins
J	J-Integral

Table C1 C(T) specimen dimensions and crack length information comparing the unloading compliance estimates to 9-point average physical measurements.

Specimen	Crack Size Information					Basic Dimensions				
	a ₀ (in)	a _{0q} (in)	a _f (in)	Δa _p (in)	Δa _{predicted} (in)	B (in)	B _N (in)	W (in)	a _N (in)	H (in)
EE-L1	0.929	0.937	1.079	0.150	0.173	0.515	0.412	2.004	0.874	2.400
EE-L2	0.969	0.953	1.488	0.520	0.524	0.515	0.412	2.005	0.874	2.400
EE-T1	0.961	0.937	1.740	0.780	0.689	0.498	0.398	2.011	0.874	2.400
EE-T2	0.988	0.957	1.701	0.713	0.669	0.514	0.411	2.003	0.874	2.400
EW-L1	0.941	0.894	1.500	0.559	0.579	0.511	0.409	2.007	0.874	2.400
EW-L2	0.941	0.902	1.512	0.571	0.575	0.511	0.409	2.014	0.874	2.400
EW-T1	0.980	0.949	1.488	0.508	0.508	0.501	0.400	2.000	0.874	2.400
EW-T2	0.988	0.953	1.728	0.740	0.650	0.497	0.398	2.002	0.874	2.400
WW-L1	0.988	0.941	1.579	0.591	0.606	0.497	0.397	2.007	0.874	2.400
WW-L2	0.961	0.925	1.500	0.539	0.559	0.494	0.395	2.009	0.874	2.400
WW-T1	1.000	0.949	1.740	0.740	0.736	0.496	0.397	2.013	0.874	2.400
WW-T2	0.988	0.953	1.642	0.654	0.606	0.499	0.399	2.007	0.874	2.400
WE-L1	1.000	0.961	1.531	0.531	0.528	0.512	0.410	2.006	0.874	2.400
WE-L2	0.969	0.921	1.520	0.551	0.547	0.513	0.410	2.003	0.874	2.400
WE-T1	0.969	0.925	1.642	0.673	0.736	0.512	0.409	2.008	0.874	2.400
WE-T2	0.980	0.937	1.720	0.740	0.736	0.513	0.410	2.004	0.874	2.400

Table C2 C(T) specimen pre-crack information at room temperature (75 F)

Specimen	a _{initial} (in)	a _{final} (in)	Slope Correlation	ΔK (ksi-in ^{1/2})	R ratio	Cycles N
EE-L1	0.913	1.000	0.9998	20.13	0.097	42,200
EE-L2	0.898	1.000	0.9997	20.19	0.102	40,300
EE-T1	0.897	1.000	0.9995	20.29	0.089	60,400
EE-T2	0.895	1.000	0.9998	20.19	0.094	39,200
EW-L1	0.951	1.000	0.9998	20.17	0.093	29,300
EW-L2	0.948	1.000	0.9997	20.15	0.091	26,200
EW-T1	0.944	1.000	0.9998	19.78	0.101	16,800
EW-T2	0.896	1.000	0.9999	15.23	0.092	119,200
WW-L1	0.910	1.000	0.9992	20.23	0.100	43,900
WW-L2	0.932	1.000	0.9998	20.15	0.093	35,700
WW-T1	0.927	1.000	0.9996	20.22	0.089	45,700
WW-T2	0.898	1.001	0.9997	20.07	0.095	37,700
WE-L1	0.894	1.000	0.9997	20.02	0.096	45,700
WE-L2	0.913	1.000	0.9998	20.06	0.092	36,800
WE-T1	0.916	1.000	0.9998	19.73	0.104	114,200
WE-T2	0.903	1.000	0.9998	20.14	0.092	41,100

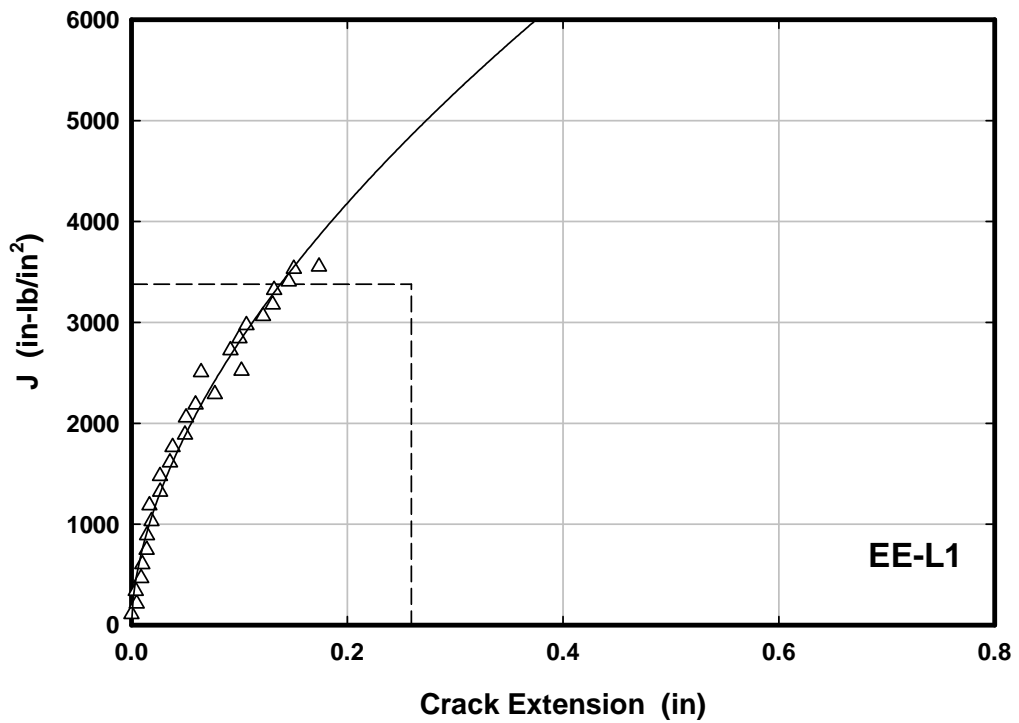
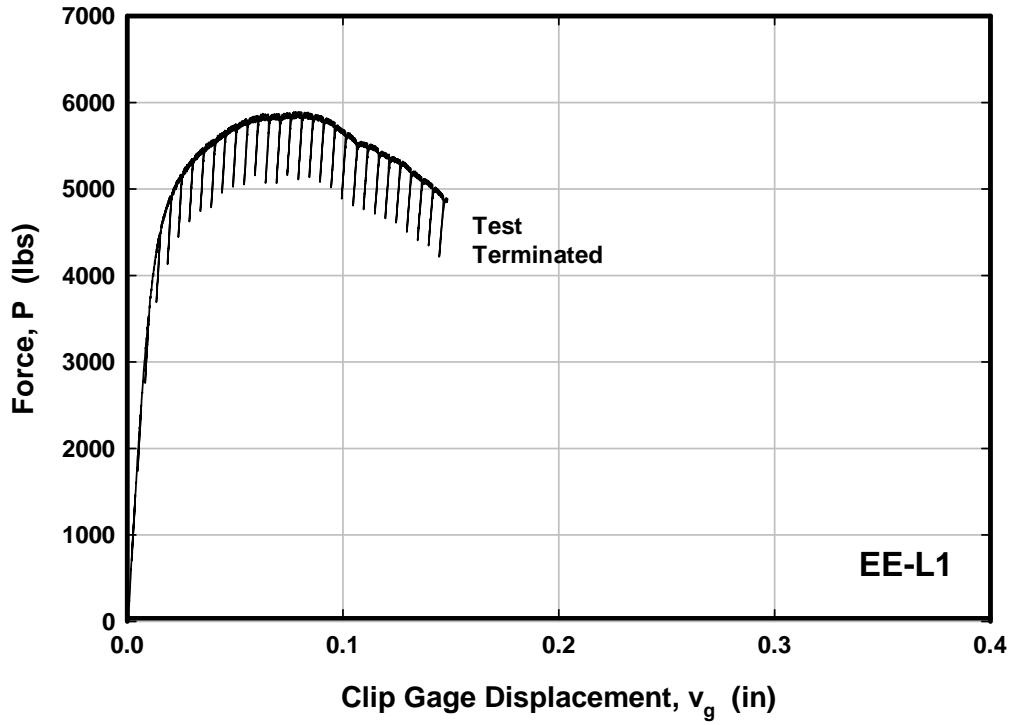


Figure C1 Load versus crack mouth opening displacement placement and J-R curve for specimen EE-L1.

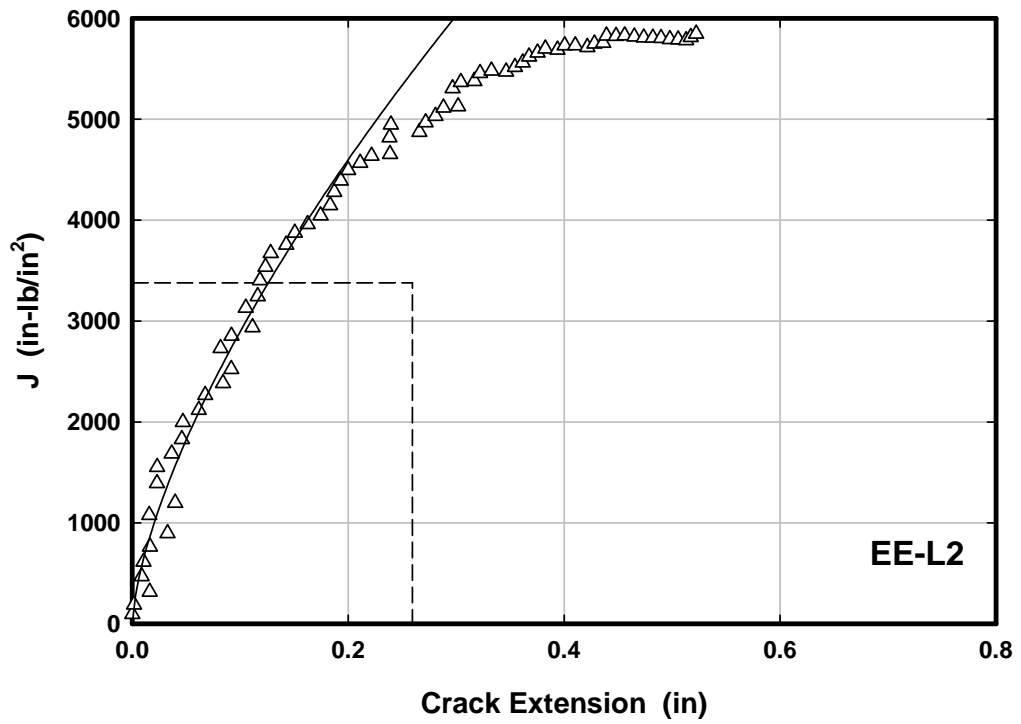
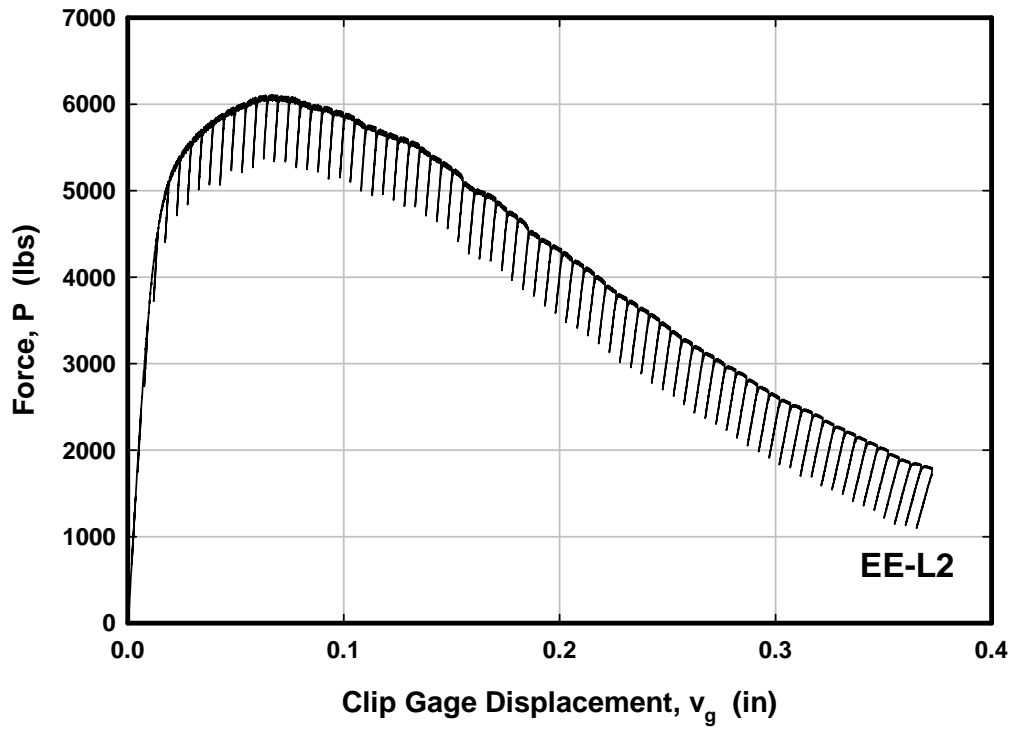


Figure C2 Load versus crack mouth opening displacement placement and J-R curve for specimen EE-L2.

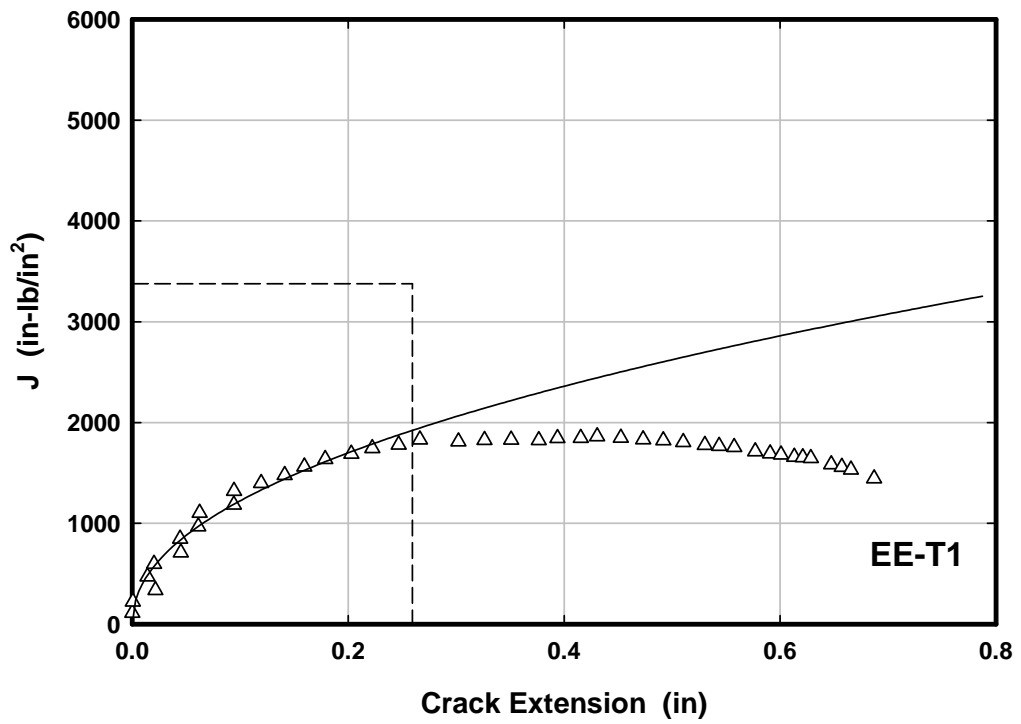
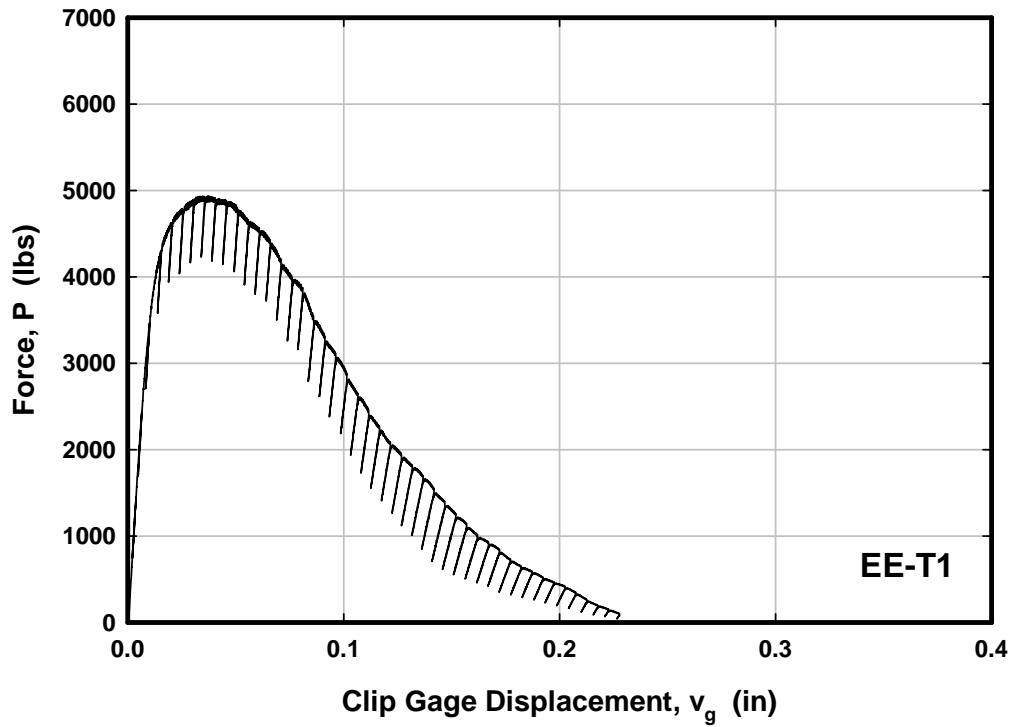


Figure C3 Load versus crack mouth opening displacement placement and J-R curve for specimen EE-T1.

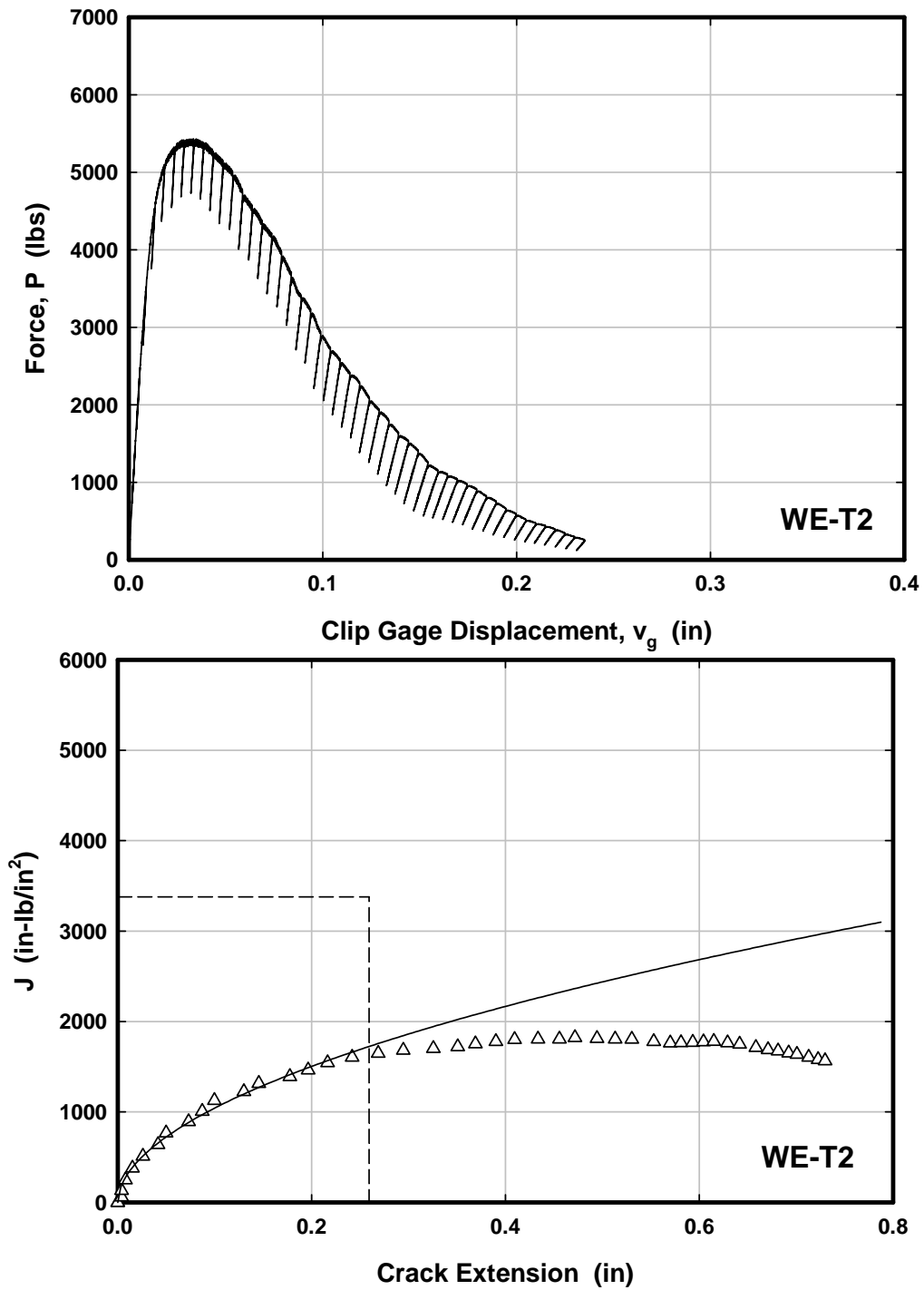


Figure C4 Load versus crack mouth opening displacement placement and J-R curve for specimen EE-T2.

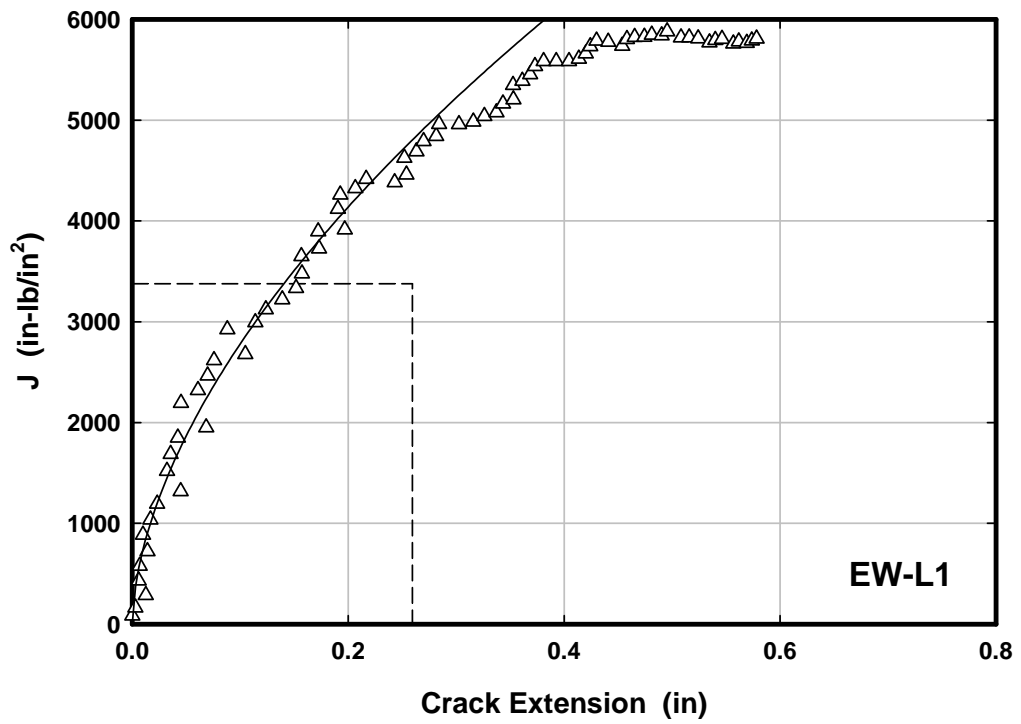
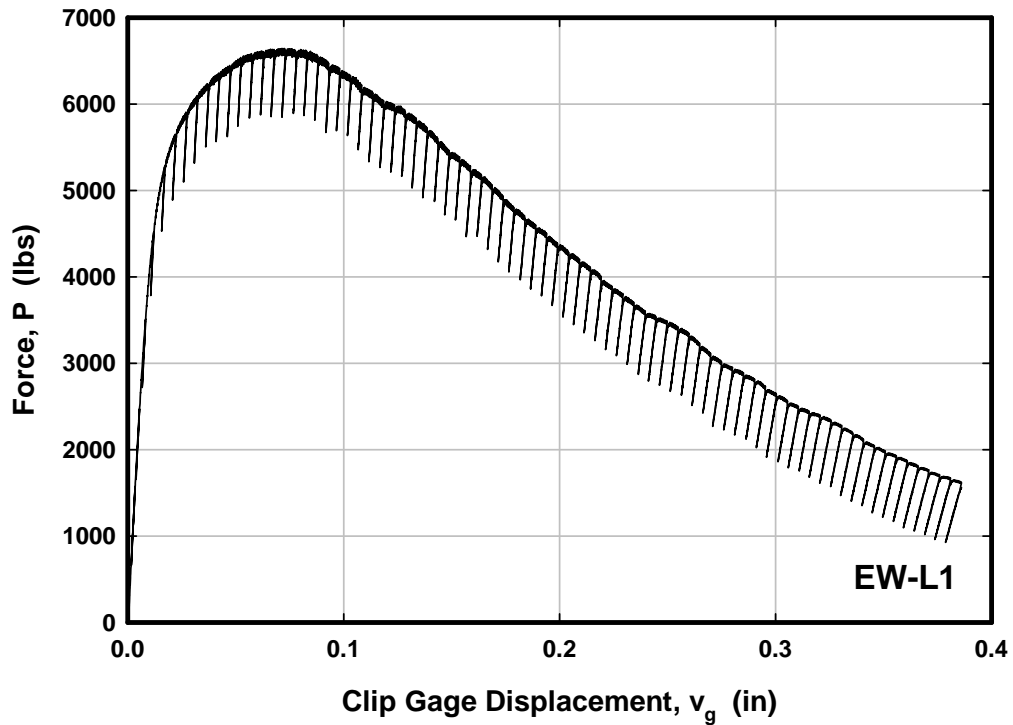


Figure C5 Load versus crack mouth opening displacement placement and J-R curve for specimen EW-L1.

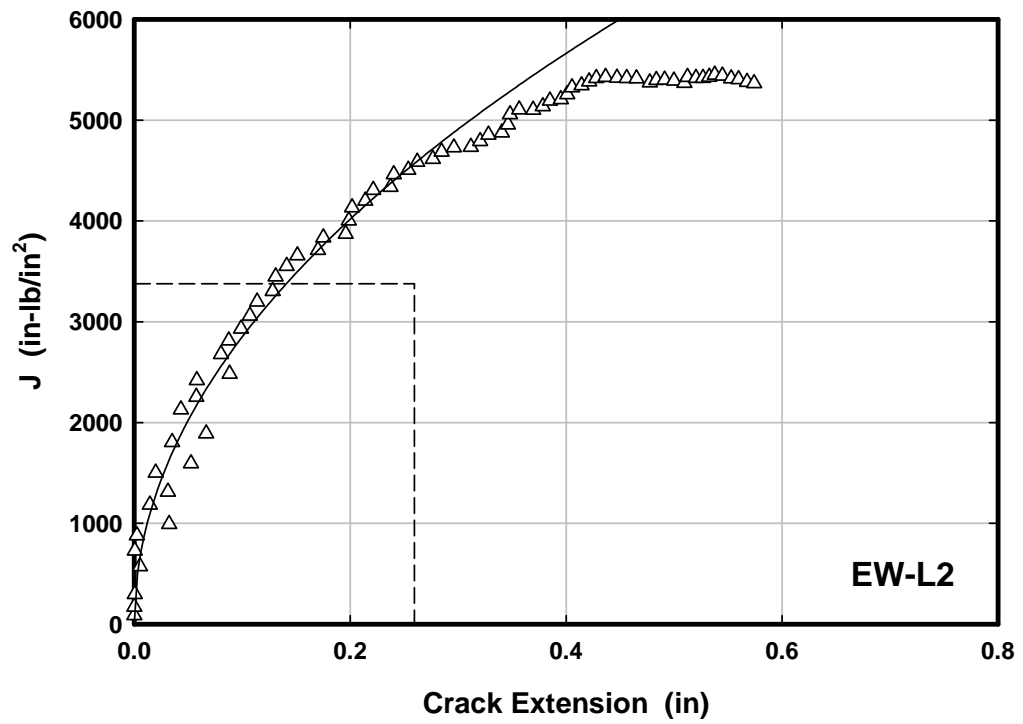
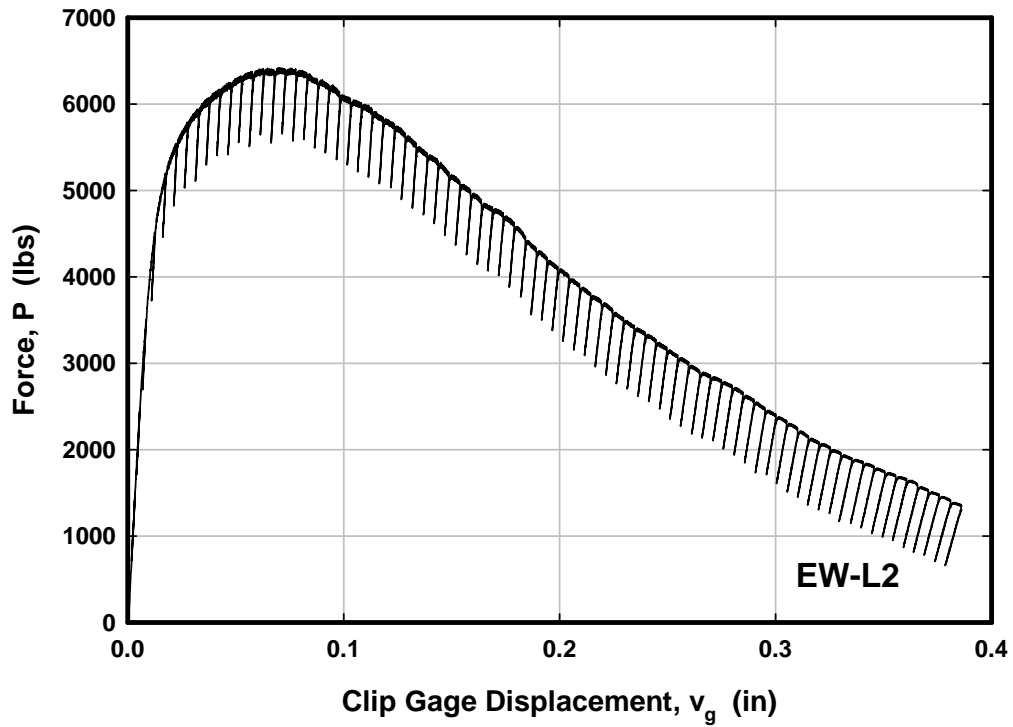


Figure C6 Load versus crack mouth opening displacement placement and J-R curve for specimen EW-L2.

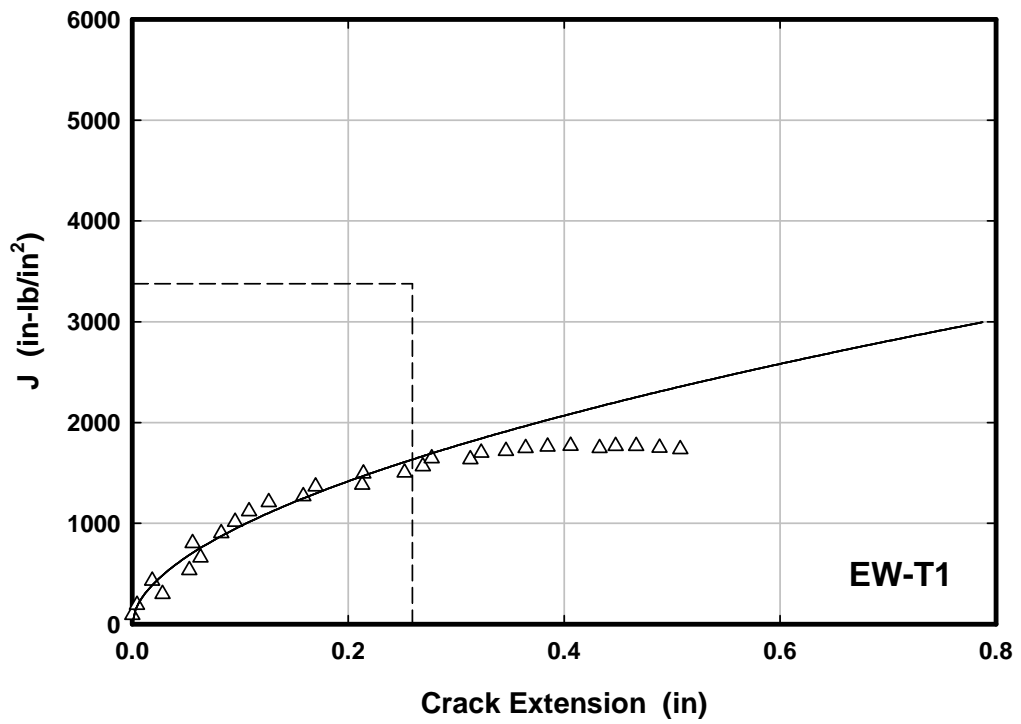
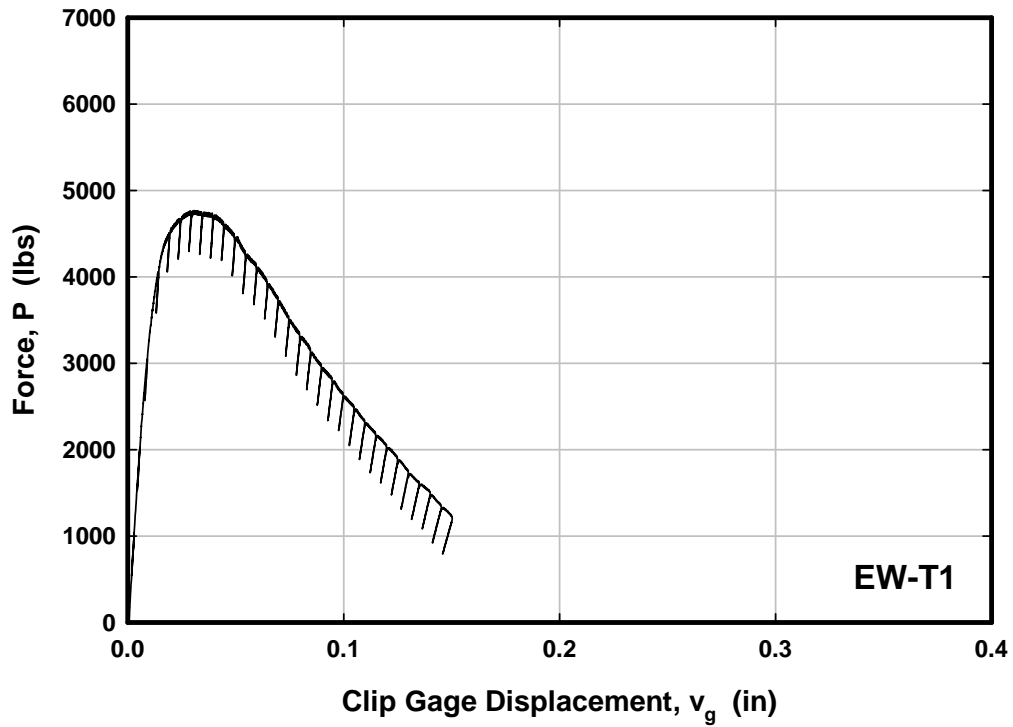


Figure C7 Load versus crack mouth opening displacement placement and J-R curve for specimen EW-T1.

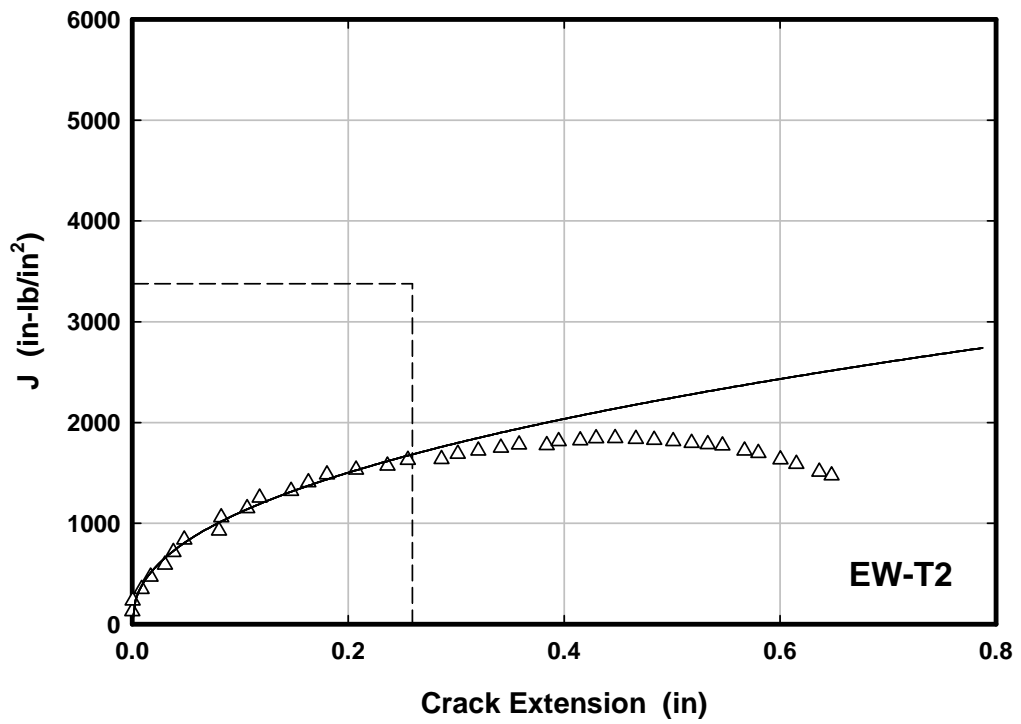
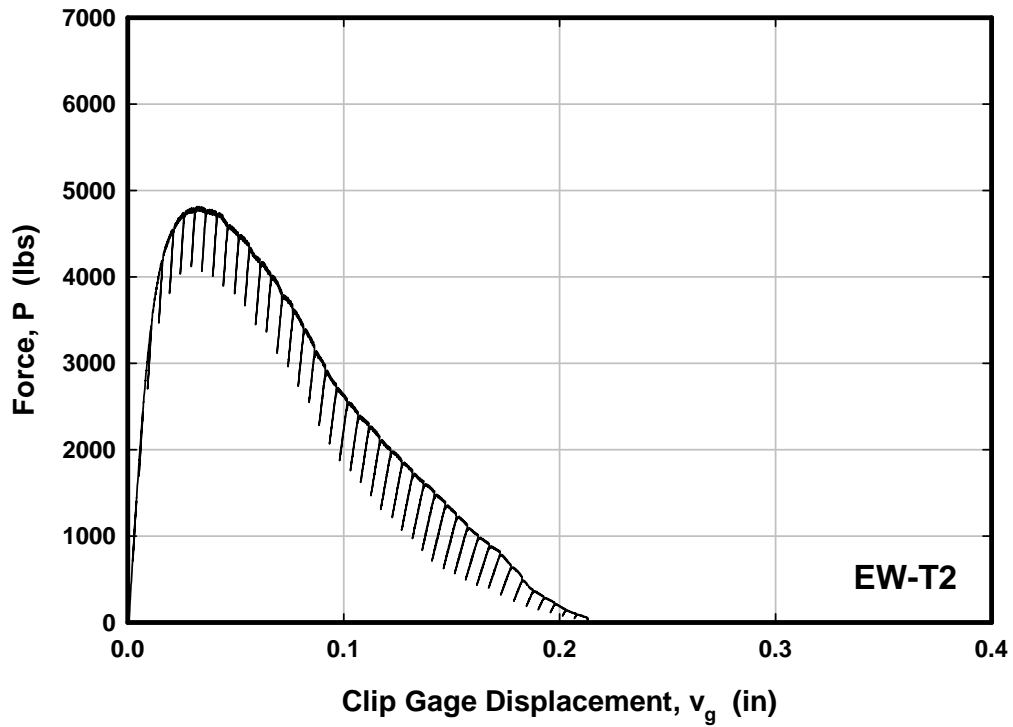


Figure C8 Load versus crack mouth opening displacement placement and J-R curve for specimen EW-T2.

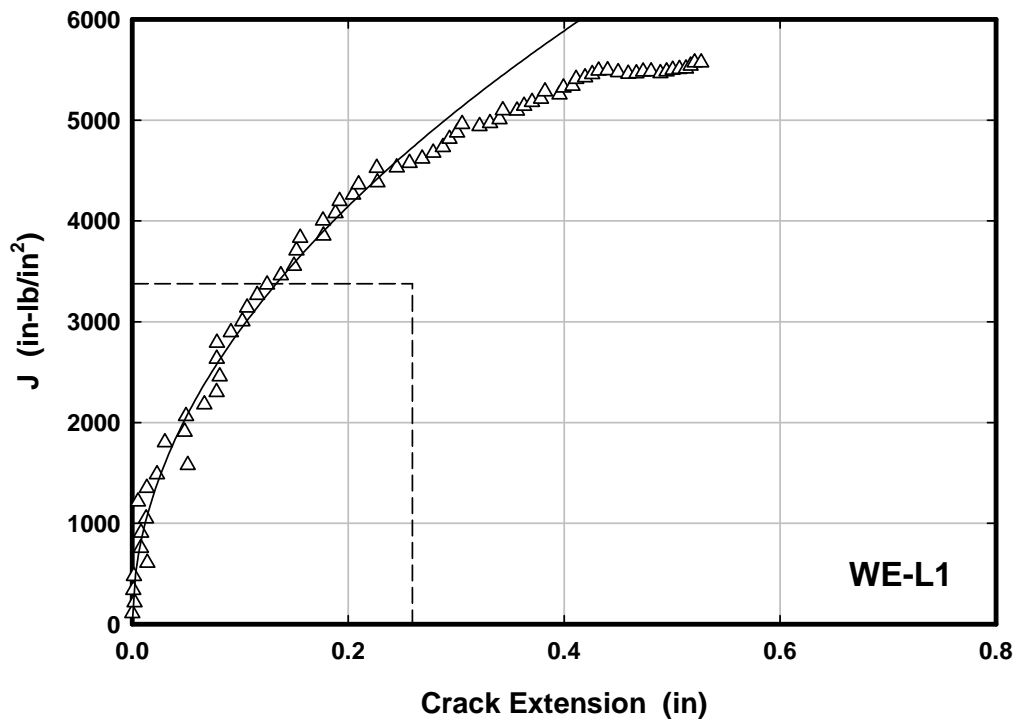
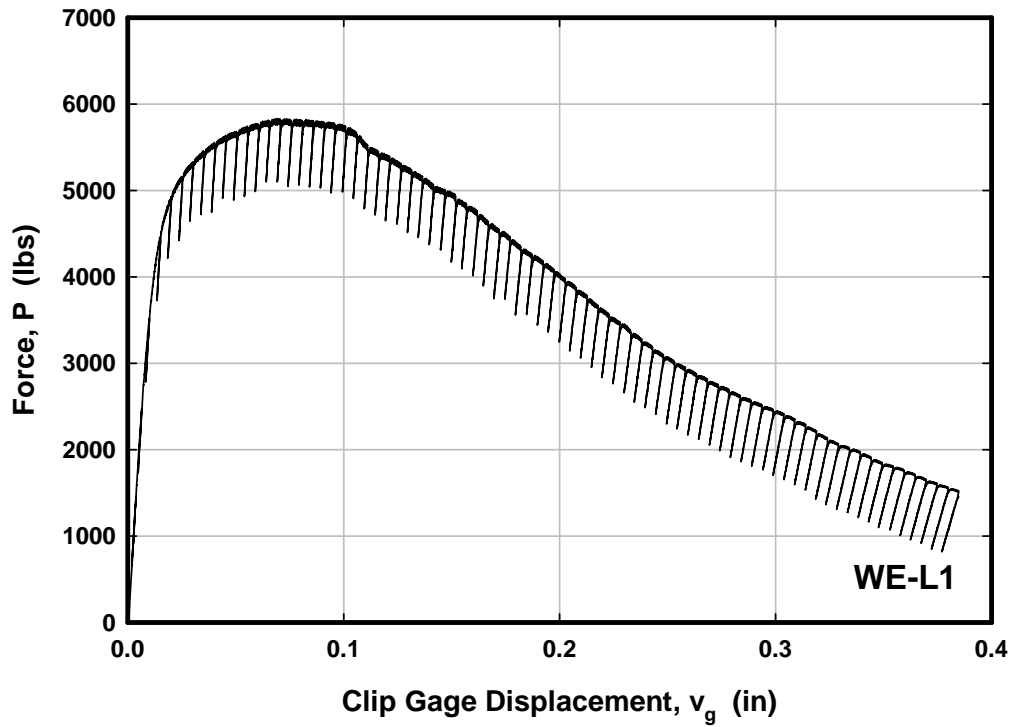


Figure C9 Load versus crack mouth opening displacement placement and J-R curve for specimen WE-L1.

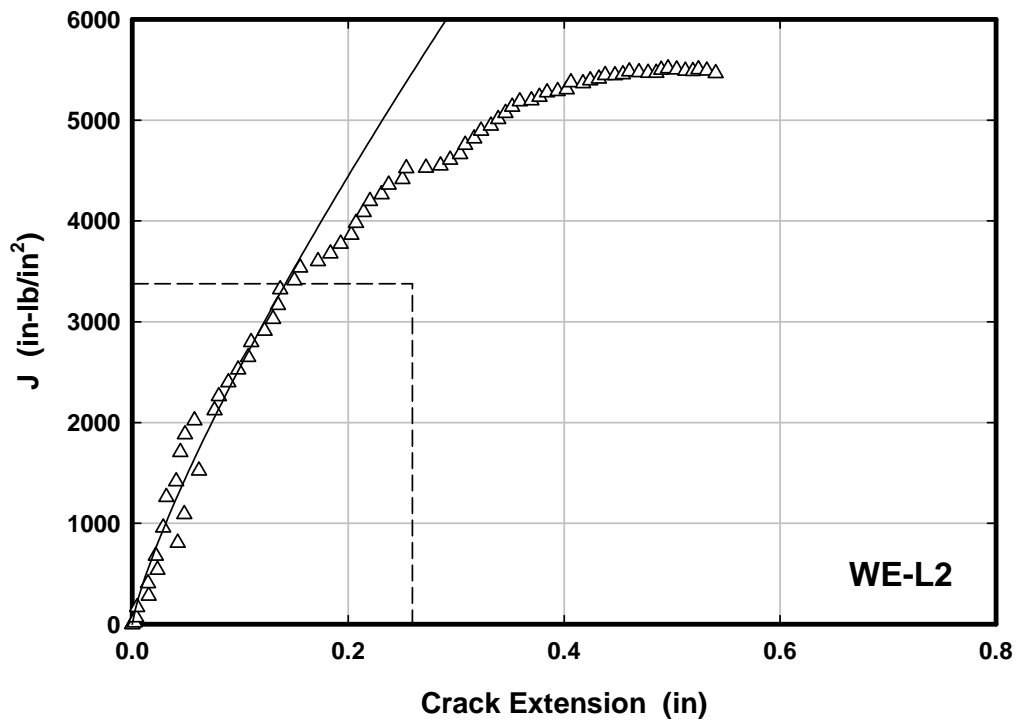
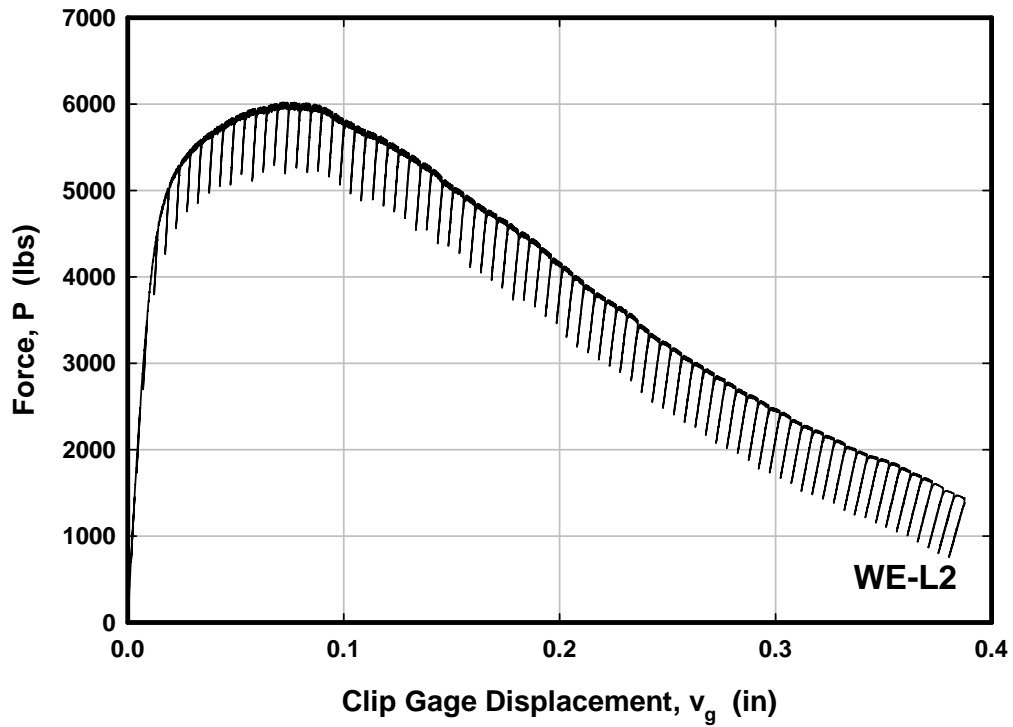


Figure C10 Load versus crack mouth opening displacement placement and J-R curve for specimen WE-L2.

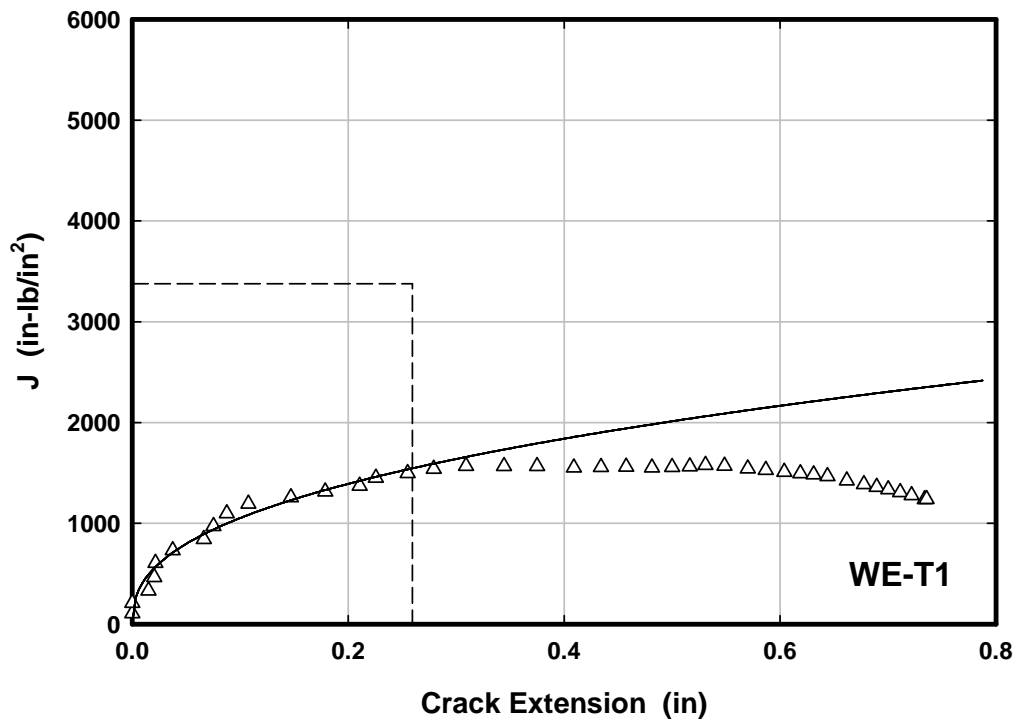
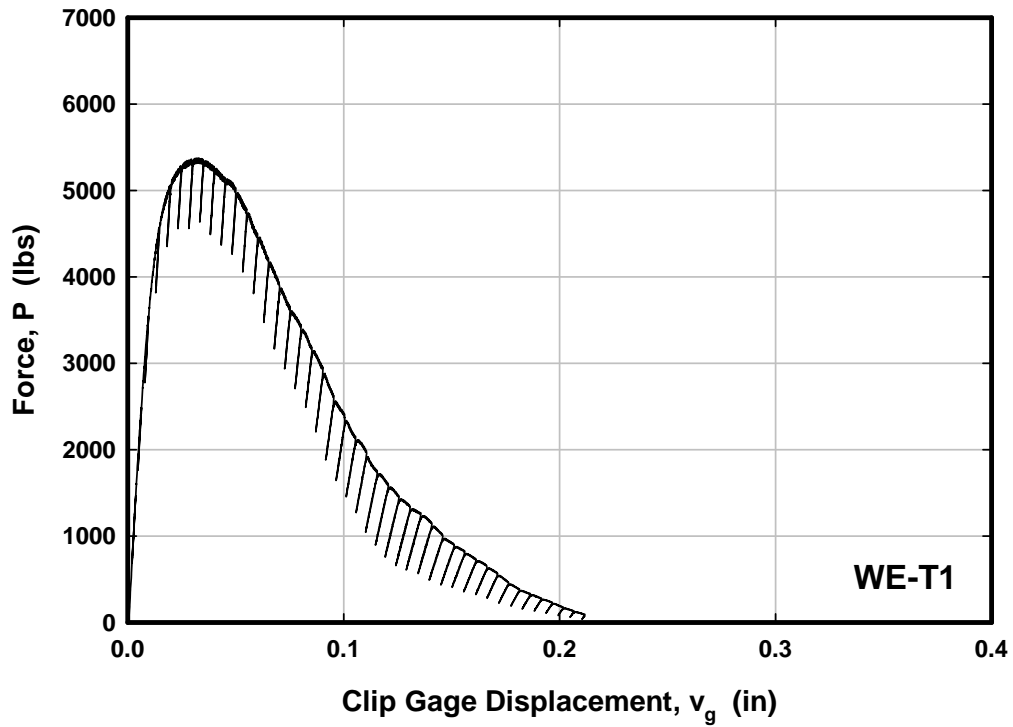


Figure C11 Load versus crack mouth opening displacement placement and J-R curve for specimen WE-T1.

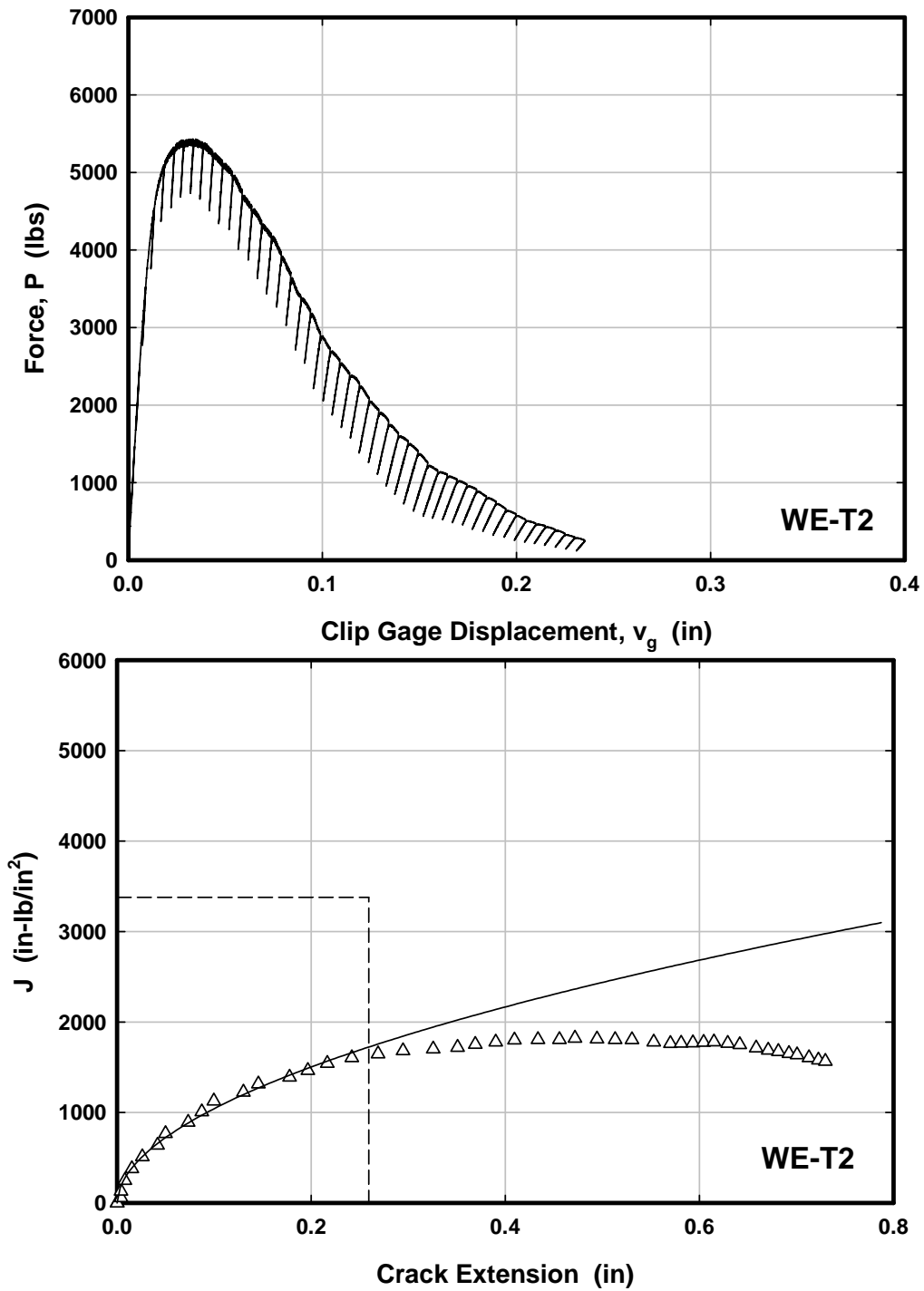


Figure C12 Load versus crack mouth opening displacement and J-R curve for specimen WE-T2.

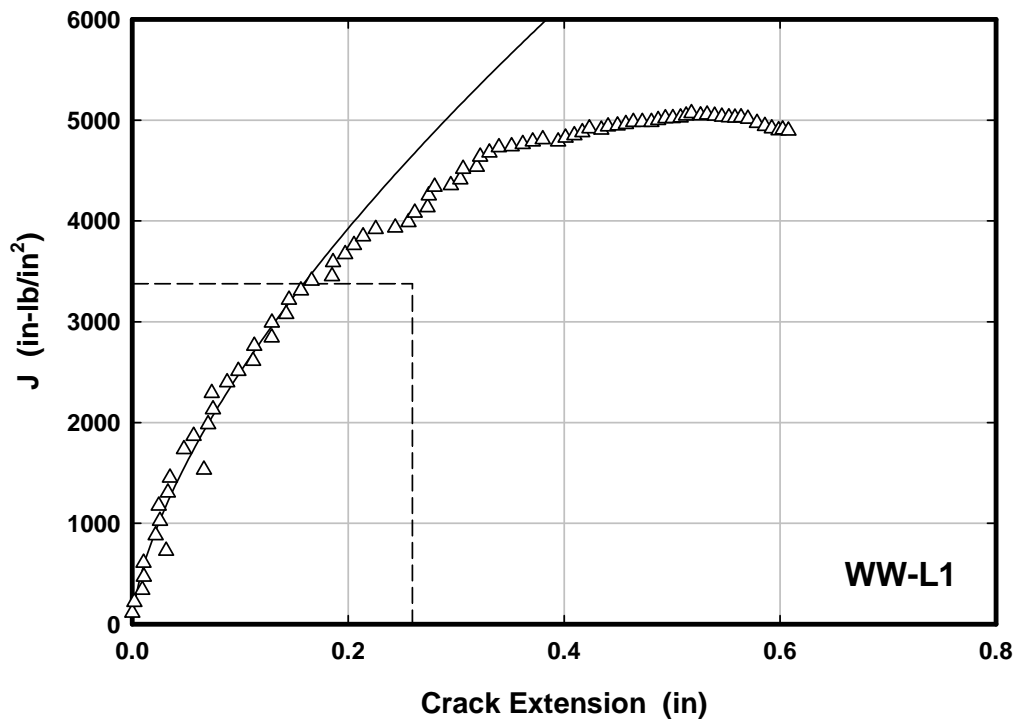
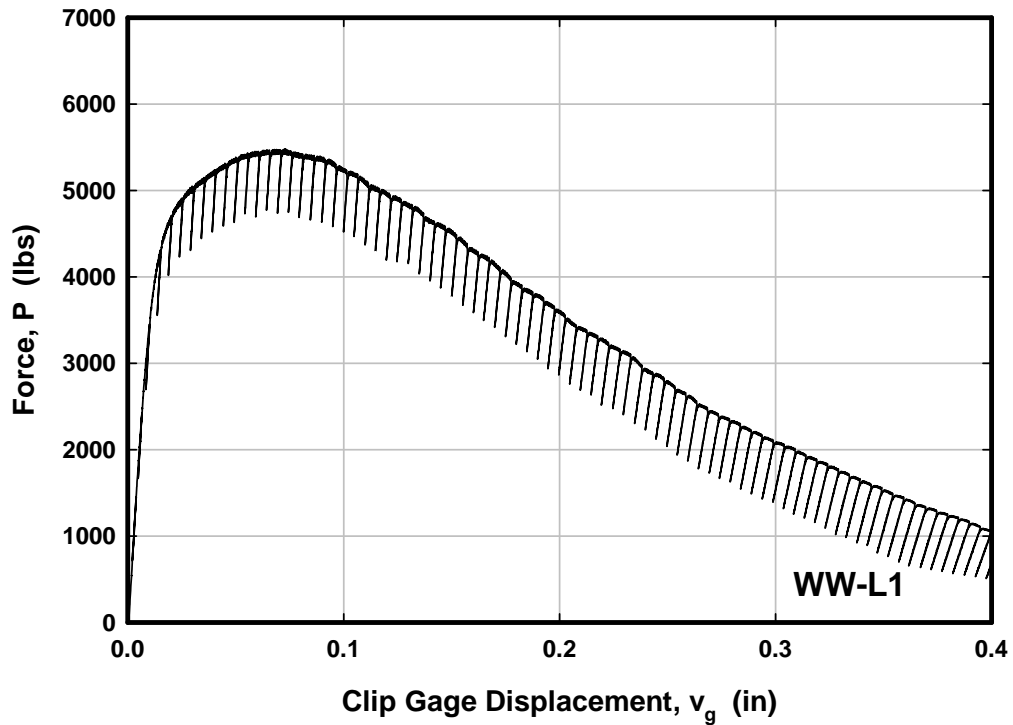


Figure C13 Load versus crack mouth opening displacement placement and J-R curve for specimen WW-L1.

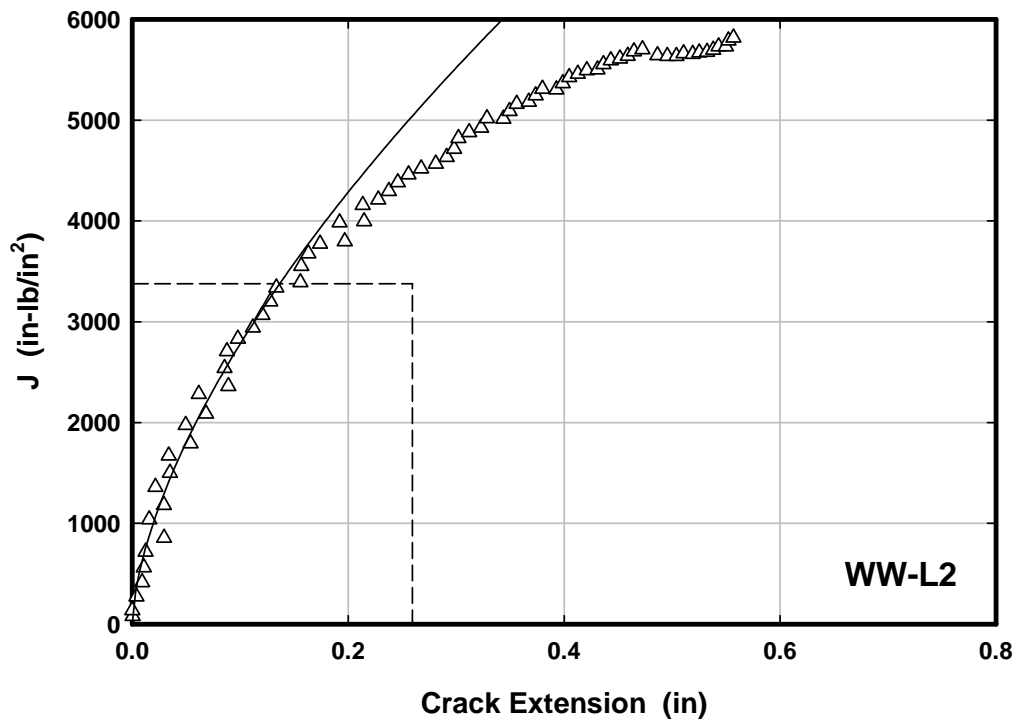
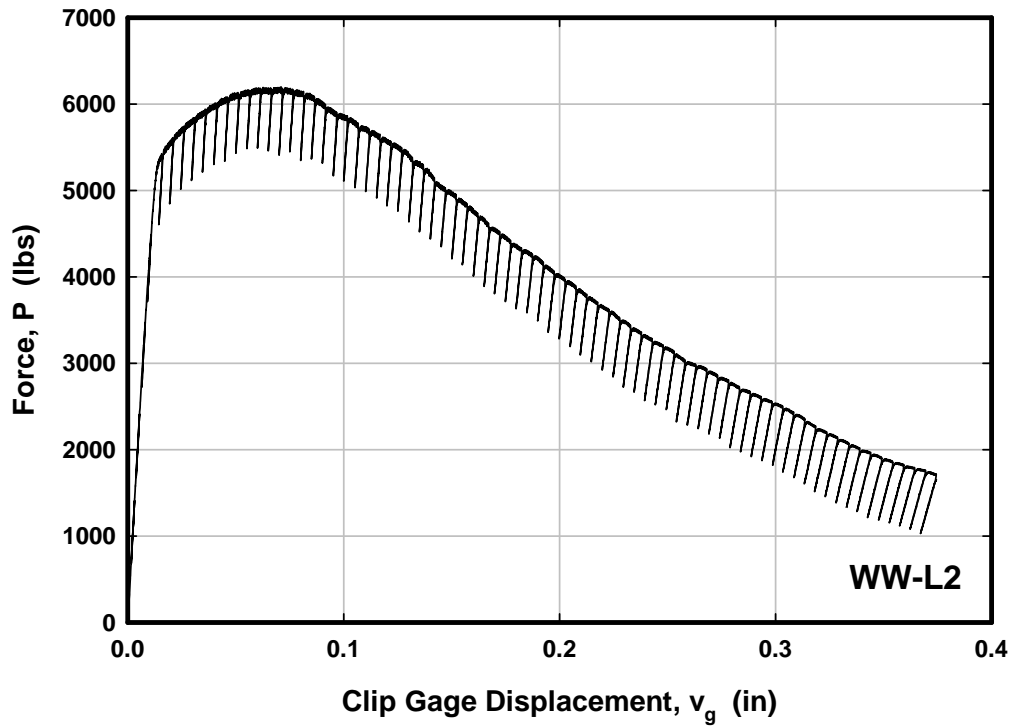


Figure C14 Load versus crack mouth opening displacement placement and J-R curve for specimen WW-L2.

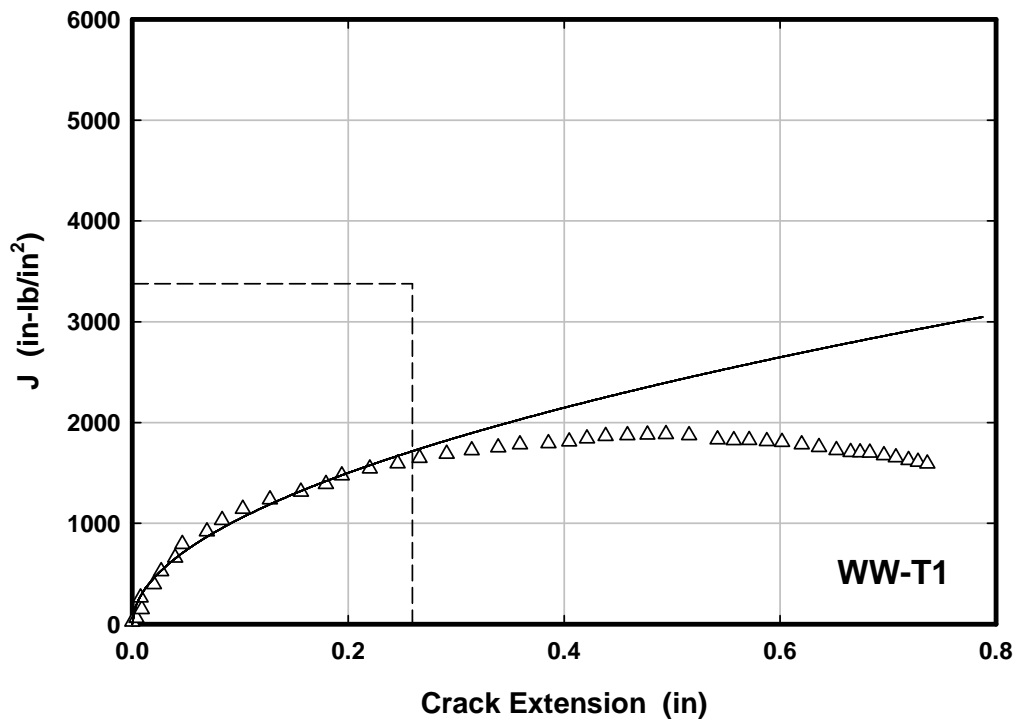
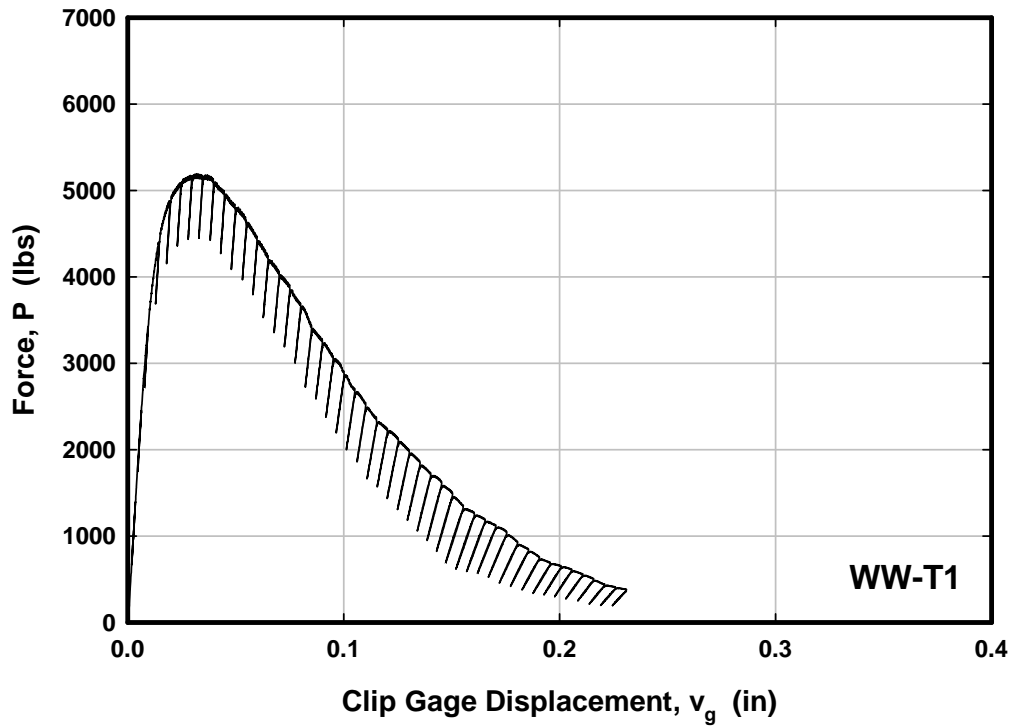


Figure C15 Load versus crack mouth opening displacement placement and J-R curve for specimen WW-T1.

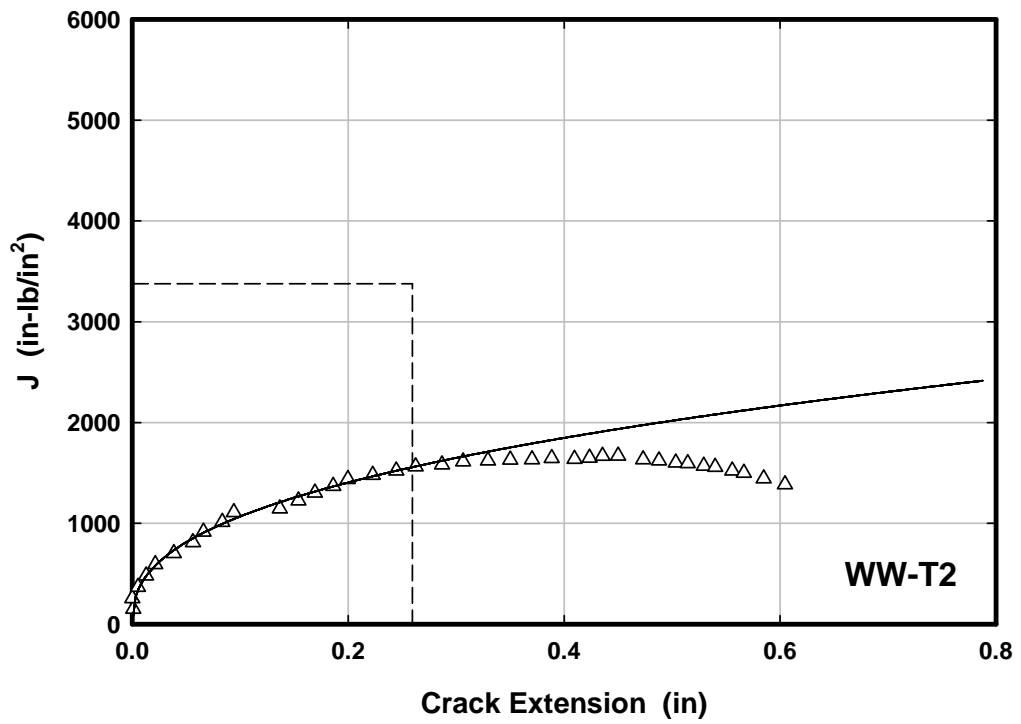
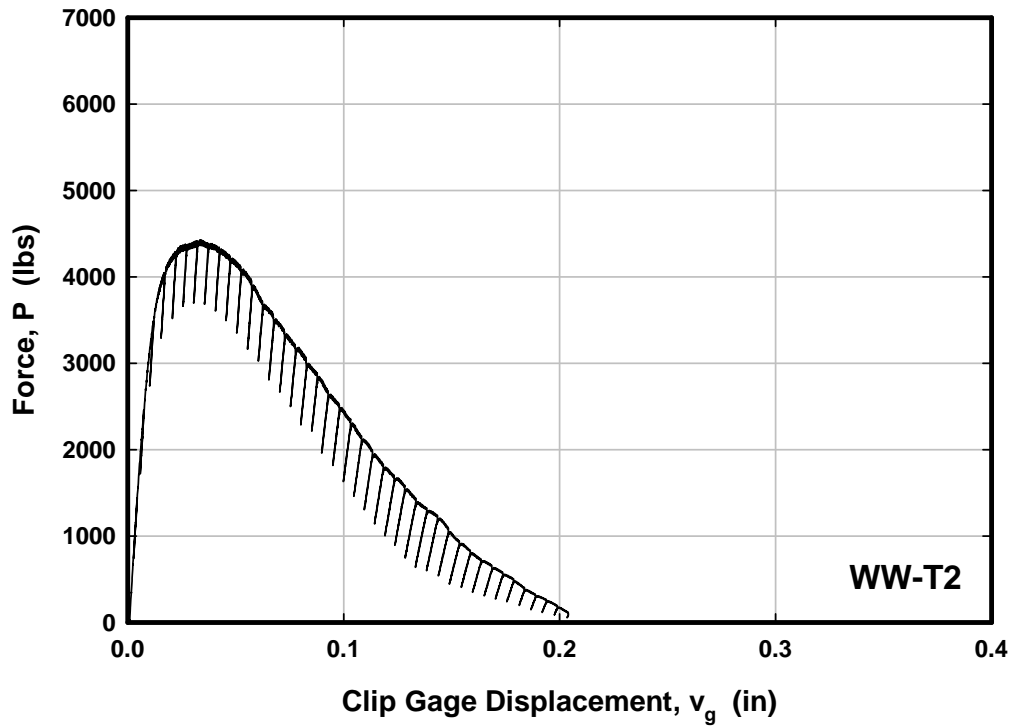


Figure C16 Load versus crack mouth opening displacement placement and J-R curve for specimen WW-T2.